(12) INTERNATIONAL APPLICATION PUBLISHED UNDER THE PATENT COOPERATION TREATY (PCT)

(19) World Intellectual Property Organization
International Bureau

(43) International Publication Date
13 October 2016 (13.10.2016)

WIPO | PCT

(10) International Publication Number
WO 2016/162801 A1

(51) International Patent Classification:
*C01G 23/047* (2006.01) *B01J 35/02* (2006.01)
*C01B 3/04* (2006.01) *B01J 35/10* (2006.01)
*B01J 35/00* (2006.01) *B01J 37/03* (2006.01)
*B01J 21/06* (2006.01) *B01J 37/08* (2006.01)
*B01J 23/755* (2006.01)

(21) International Application Number:
PCT/IB2016/051946

(22) International Filing Date:
6 April 2016 (06.04.2016)

(25) Filing Language: English

(26) Publication Language: English

(30) Priority Data:
62/144,723 8 April 2015 (08.04.2015) US

(71) Applicant: **SABIC GLOBAL TECHNOLOGIES B.V.** [NL/NL]; Plasticslaan 1, 4612 PX, Bergen op Zoom (NL).

(72) Inventors: **WATERHOUSE, Geoff. CHEN, Wan-Ting. SUN-WATERHOUSE, Dongxiao. IDRISS, Hicham.**

(81) Designated States *(unless otherwise indicated, for every kind of national protection available)*: AE, AG, AL, AM, AO, AT, AU, AZ, BA, BB, BG, BH, BN, BR, BW, BY, BZ, CA, CH, CL, CN, CO, CR, CU, CZ, DE, DK, DM, DO, DZ, EC, EE, EG, ES, FI, GB, GD, GE, GH, GM, GT, HN, HR, HU, ID, IL, IN, IR, IS, JP, KE, KG, KN, KP, KR, KZ, LA, LC, LK, LR, LS, LU, LY, MA, MD, ME, MG, MK, MN, MW, MX, MY, MZ, NA, NG, NI, NO, NZ, OM, PA, PE, PG, PH, PL, PT, QA, RO, RS, RU, RW, SA, SC, SD, SE, SG, SK, SL, SM, ST, SV, SY, TH, TJ, TM, TN, TR, TT, TZ, UA, UG, US, UZ, VC, VN, ZA, ZM, ZW.

(84) Designated States *(unless otherwise indicated, for every kind of regional protection available)*: ARIPO (BW, GH, GM, KE, LR, LS, MW, MZ, NA, RW, SD, SL, ST, SZ, TZ, UG, ZM, ZW), Eurasian (AM, AZ, BY, KG, KZ, RU, TJ, TM), European (AL, AT, BE, BG, CH, CY, CZ, DE, DK, EE, ES, FI, FR, GB, GR, HR, HU, IE, IS, IT, LT, LU, LV, MC, MK, MT, NL, NO, PL, PT, RO, RS, SE, SI, SK, SM, TR), OAPI (BF, BJ, CF, CG, CI, CM, GA, GN, GQ, GW, KM, ML, MR, NE, SN, TD, TG).

**Declarations under Rule 4.17**:

— *as to applicant's entitlement to apply for and be granted a patent (Rule 4.17(ii))*

*[Continued on next page]*

(54) Title: PHOTOACTIVE CATALYST BASED ON NON-PRECIOUS METALS DEPOSITED ON TITANIUM DIOXIDE

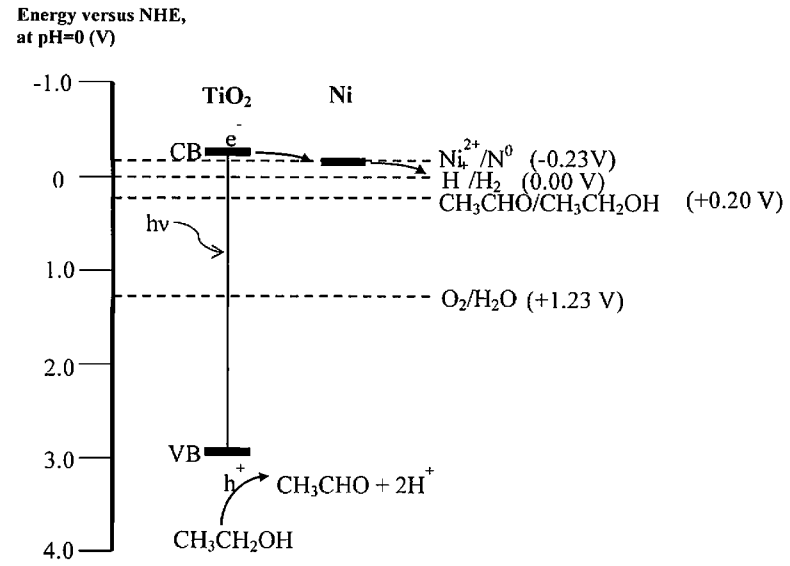


FIG. 1

(57) Abstract: Photocatalysts and methods of using photocatalysts for synergistic production of hydrogen from water are disclosed. The photocatalysts include photoactive titanium dioxide particles having nickel(0) dispersed on titanium dioxide support, the nickel catalyst having a nickel(0) content of greater than 0 to 4 wt.% as determined by X-ray fluorescence (XFR) and the nickel(0) is dispersed on the titanium dioxide support in the form of particles having an average particle size of less than or equal to 1 nm.

WO 2016/162801 A1

**Published**:

— *with international search report (Art. 21(3))*

— *before the expiration of the time limit for amending the claims and to be republished in the event of receipt of amendments (Rule 48.2(h))*

# PHOTOACTIVE CATALYST BASED ON NON-PRECIOUS METALS DEPOSITED ON TITANIUM DIOXIDE

## CROSS REFERENCE TO RELATED APPLICATIONS

[0001] This application claims the benefit of priority of U.S. Provisional Patent Application No. 62/144,723, filed April 8, 2015, which is hereby incorporated by reference in its entirety.

## BACKGROUND OF THE INVENTION

### A. Field of the Invention

[0002] The invention generally concerns photocatalysts that include non-precious metals dispersed on a titanium dioxide support. In particular, the invention concerns nickel(0) dispersed on a titanium dioxide support in the form of particles having an average particle size of less than or equal to 1 nm.

### B. Description of Related Art

[0003] Hydrogen production from water offers enormous potential benefits for the energy sector, the environment, and the chemical industry. While methods currently exist for producing hydrogen and oxygen from water, many of these methods can be costly, inefficient, or unstable. For instance, photoelectrochemical (PEC) water splitting requires an external bias or voltage and a costly electrode (e.g., Pt-based).

[0004] With respect to photocatalytic electrolysis of water from light sources, while many advances have been achieved in this area, most materials are either unstable under realistic water splitting conditions or require considerable amounts of other components (e.g., large amounts of sacrificial hole or electron scavengers) to work, thereby offsetting any gained benefits. By way of example, a semiconductor photocatalyst is a material that can be excited upon receiving energy equal to or higher than its electronic band gap. Upon photo-excitation, electrons are transferred from the valence band (VB) to the conduction band (CB), resulting in the formation of an excited electron (in the CB) and a hole (in the VB). In the case of water splitting, electrons in the CB reduce hydrogen ions to $H_2$ and holes in the VB oxidize oxygen ions to $O_2$. One of the main limitations of most photocatalysts is the fast electron-hole recombination, a process that occurs at the nanosecond scale, while the oxidation-reduction reactions are much slower (microsecond time scale). Over 90% of photo-excited

electron-hole pairs disappear before reaction by radiative and non-radiative decay mechanisms. To increase the electron life time metal deposition on the semiconductor surfaces are routinely used while organic compounds such as alcohols and glycols are added to the aqueous media to increase the hold lifetime. Current photocatalysts such as those that utilize photoactive materials having deposited noble metals are very expensive to manufacture and, thus, make commercialization of such photocatalysts ineffective.

**[0005]** There have been many attempts to make non-noble metal photocatalysts as effective as noble metal photocatalysts. For example, Yoshinaga *et al.*, in *J. Colloid and Interface Science*, 2007, Vol. 39 attempts to make a photocatalyst by depositing metallic nickel using chemical vapor reductive deposition on a titania thin film. Russian Patent No. 2275238 describes a three step process to make a photocatalyst containing at least 30% crystalline anatase phase and 0.5 to 2 wt.% of nickel having a mean pore diameter of 2 to 16 nm and a surface area of at least 70 $m^2/g$. The support is made through a sol-gel process, which is then impregnated with nickel salt solution. The impregnated catalyst is then reduced using sodium borohydride. Kimijima *et al.* in *Chem Lett.*, 2010, Vol. 39, also uses a sol-gel method to prepare titanium dioxide nanoparticles and then loads the nanoparticles with 0.5 wt.% nickel using liquid-phase reductive deposition methods. This cubic shaped catalyst produced hydrogen at a rate of 600 $\mu L\ h^{-1}$. Korzhak *et al.* in *Theoretical and Experimental Chemistry*, 2005, Vol. 41 describes a sol-gel precipitation method to prepare mesoporous titanium dioxides which was irradiated in the presence of $NiClO_4$ to generate hydrogen. Singh *et al.* in *AIP Conference Proceedings*, Sep. 2012, Vol 1482, Issue 1, describes preparation of a series of a 2, 5 and 10 wt.% Ni on TiO2 catalysts using wet impregnation methods. Tran *et al.* in *Phys. Chem. Chem. Phys.* 2012, Vol 14, describes depositing nickel ions in the form of nickel nitrate onto a single anatase phase titanium dioxide substrate and then reducing the nickel ions to metallic nickel using sodium borohydride. The resulting $Ni/TiO_2$ catalysts had elongated nickel nanoclusters having a width of 1-2 nm and a length of about 20 nm. deposited on the surface of the titanium dioxide substrate.

**[0006]** The catalysts prepared by the above described methods all suffer in that they produce hydrogen at a rate significantly lower than noble metal doped titanium dioxide photocatalysts, require elevated amounts of transition metals to be effective, involve labor intensive preparation methods, and/or result in transition metals being agglomerated on the surface of the titanium dioxide.

## SUMMARY OF THE INVENTION

**[0007]** A discovery has been made that provides a solution to the aforementioned problems associated with conventional photocatalysts. The discovery is premised on a semiconductor photocatalyst that can efficiently harvest solar energy and generate $H_2$ from water or biofuels by using cost-efficient nonprecious metals. This can provide a cost-effective alternative to conventional photocatalysts that contain noble metals (e.g., M/$TiO_2$ (M = Pd, Pt or Au)). The low cost, highly reactive photocatalysts of the present invention include nickel(0) or $Ni^0$ metal at 0 < 4 wt. % metal loading on a $TiO_2$ support (e.g., biphasic anatase/rutile support such as P25). The $Ni^0$ is highly dispersed over the support in the form of particles having an average particle size or diameter of $\leq$ 1 nm or less than 1 nm. The particles, in preferred aspects, are substantially spherical or semi-spherical in shape. The photocatalyst can be used in water-splitting reactions that contain a sacrificial agent. It was surprisingly found that the photocatalyst of the present invention was capable of producing hydrogen ($H_2$) from water at a faster rate than a noble metal titanium dioxide microparticle photocatalyst when the sacrificial agent to water volume ratio was less than 20:80 under the same UV conditions (*See*, for example, Example 3). Without wishing to be bound by theory, it is believed that the high activity at low ethanol concentrations can be attributed to the very high dispersion of nickel(0) particles on the surface of the titanium dioxide substrate. Further, it is believed that the particle size of less than or equal to 1 nm allows for this high dispersion and further allows for the use of low amounts of $Ni^0$ metal loading (e.g., 0 < 4 wt. %), thereby providing a cost-efficient and effective alternative to the currently available conventional catalysts.

**[0008]** In one aspect of the present invention, there is disclosed a photocatalyst that includes Ni(0) dispersed on titanium dioxide ($TiO_2$) support. The Ni(0) is dispersed on the surface of the titanium dioxide support in the form of particles having an average particle size of less than or equal to 1 nm, preferably less than 1 nm. The photocatalyst can have a Ni(0) content of greater than 0 to 4 wt.%, or 0.1 to 4 wt.%, preferably 0.2 to 2 wt. %, or more preferably 0.4 to 0.8 wt.%, or most preferably 0.4 to 0.6 wt.% as determined by X-ray fluorescence (XRF). The Ni(0) to Ti atom percentage can range from greater than 0 to 0.07 or from 0.03 to 0.04. A Brunauer-Emmett-Teller (BET) surface area of the photocatalyst may be 43 to 46 $m^2g^{-1}$. The Ni(0) particles can be obtained, *in situ*, from $H_2$ reduction of a Ni(II) complex, preferably nickel oxide (NiO). The $TiO_2$ support may include anatase and rutile phases. The ratio of anatase to rutile can range from 1.5:1 to 10:1, preferably 3:1 to

8:1, and most preferably from 5:1 to 7:1. In another aspect, the titanium dioxide support can be single phase anatase. The photocatalyst can be in particulate or powdered form. The photocatalyst can be self-supported or can be supported by a substrate such as glass, polymer beads, or a metal oxide. In one particular aspect, the photocatalyst does not include any one of gold, ruthenium, rhenium, rhodium, palladium, silver, copper, osmium, iridium, and platinum.

**[0009]** The photocatalysts of the present invention are capable of splitting water in combination with a light source. No external bias or voltage is needed to efficiently split water. The hydrogen production rate from water can be modified as desired by subjecting the system to different amounts of light or light flux. In some embodiments, the water undergoing the water-splitting reaction can include the photocatalyst of the present invention, a sacrificial agent, or both. The sacrificial agent can be methanol, ethanol, propanol, iso-propanol, n-butanol, iso-butanol, ethylene glycol, propylene glycol, glycerol, oxalic acid, trimethyl amine, triethanolamine, or any combination thereof. In one aspect, the sacrificial agent is ethanol. The composition can include a sacrificial agent to water volume ratio of less than 20:80, preferably from 1:99 to 15:85, or more preferably from 1:99 to 10:90. With a light source, the photocatalysts of the present invention can be used in water splitting systems that include a sacrificial agent to provide a hydrogen production rate from water 2 to 12 $mmol/g_{Catal}$ hour, preferably 5 to 12 $mmol/g_{Catal}$ hour, and most preferably from 10 to 12 $mmol/g_{Catal}$ hour using a light source having a flux from about 0.1 to 10 $mW/cm^2$ at 360 nm.

**[0010]** In another aspect of the present invention, there is disclosed a system for producing hydrogen gas and/or oxygen gas from water. The system can include a container (e.g., transparent or translucent containers or opaque containers such as those that can magnify light (e.g., opaque container having a pinhole(s)) and a composition that includes photocatalyst of the present invention, water, and optionally a sacrificial agent. The container in particular embodiments is transparent or translucent. The system can also include a light source for irradiating the composition. The light source can be natural sunlight or can be from a non-natural or artificial source such as a UV lamp or an UV-visible lamp. While the system may use an external bias or voltage, such an external bias or voltage is not needed due to the efficiency of the photocatalysts of the present invention.

**[0011]** Also disclosed is a method of making the photocatalysts. The method can include the steps of (a) obtaining a titanium dioxide support material having a Ni(II) complex dispersed on the support material and (b) heating the titanium dioxide support material and

reducing the Ni(II) to Ni(0) with a gas containing $H_2$ to form the photocatalyst. The Ni(II) complex in step (b) can be NiO. The gas containing hydrogen can include inert gas (e.g., nitrogen or argon). The titanium dioxide support material can be heated at a temperature of 350 °C to 700 °C for at least one hour or at a temperature of 450 °C to 550 °C for 1 to 3 hours or for 2 hours. Obtaining the titanium dioxide support material can include forming the Ni(II) complex on the support material. A nickel (II) salt and glycerol can be combined with water to form an aqueous solution of a Ni(II)-glycerol complex. Titanium dioxide support material can be added to the solution. A basic media can be added to the solution to precipitate the Ni(II)-glycerol complex on the titanium dioxide support material and form a mixture. The precipitation can be performed by adding (e.g., dropwise) an aqueous solution of base with stirring until a pH of about 12 is obtained. After a pH of 12 is reached, the mixture can be further agitated for a desired amount of time (for example, 1 hour). All or substantially all the liquids can be removed from the mixture and the solids can be collected and washed. The resulting solids can include $Ni(OH)_2/TiO_2$. The washed solids can be dried and calcined to form NiO. Calcining can include heating the dried solids to a temperature of 300 °C for two hours in the presence of oxygen (e.g. air).

**[0012]** In the context of the present invention, there are 40 embodiments described. The first embodiment describes a photocatalyst that includes Ni(0) dispersed on a titanium dioxide support, said photocatalyst having a Ni(0) content of greater than 0 to 4 wt. %, as determined by X-ray fluorescence (XRF), wherein the Ni(0) is dispersed on the titanium dioxide support in the form of particles having an average particle size of less than or equal to 1 nm. Embodiment 2 is the photocatalyst of embodiment 1, wherein the photocatalyst has a Brunauer-Emmett-Teller (BET) surface area of 43 to 46 $m^2g^{-1}$. Embodiment 3 is the photocatalyst of any one of embodiments 1 or 2, wherein the photocatalyst has a Ni(0) to Ti atom % of greater than 0 to 0.07, as determined by X-ray photoelectron spectroscopy (XPS). Embodiment 4 is the photocatalyst of any one of embodiments 1 to 3, wherein the Ni(0) content is 0.1 to 4 wt. %, preferably 0.2 to 2 wt. %, or more preferably 0.4 to 0.8 wt.%, or most preferably 0.4 to 0.6 wt. %. Embodiment 5 is the photocatalyst of embodiment 4, wherein the Ni(0):Ti atom % is 0.03 to 0.04. Embodiment 6 is the photocatalyst of any one of embodiments 1 to 5, wherein the Ni(0) is obtained, *in situ*, from $H_2$ reduction of a Ni(II) complex. Embodiment 7 is the photocatalyst of embodiment 6, wherein the Ni(II) complex is NiO. Embodiment 8 is the photocatalyst of any one of embodiments 1 to 7, wherein the titanium dioxide includes anatase, rutile, brookite, or any combination thereof. Embodiment

9 is the photocatalyst of embodiment 8, wherein the titanium dioxide support includes anatase and rutile. Embodiment 10 is the photocatalyst of embodiment 9, wherein the ratio of anatase to rutile ranges from 1.5:1 to 10:1, preferably 3:1 to 8:1, and most preferably from 5:1 to 7:1. Embodiment 11 is the photocatalyst of embodiment 8, wherein the titanium dioxide support includes single phase anatase. Embodiment 12 is the photocatalyst of any one of embodiments 1 to 11, wherein the photocatalyst is in particulate or powdered form. Embodiment 13 is the photocatalyst of any one of embodiments 1 to 12, wherein the photocatalyst does not include any one of gold, ruthenium, rhenium, rhodium, palladium, silver, copper, osmium, iridium, and platinum. Embodiment 14 is the photocatalyst of any one of embodiments 1 to 13, wherein the photocatalyst is self-supported. Embodiment 15 is the photocatalyst of any one of embodiments 1 to 13, wherein the photocatalyst is supported by a substrate such as glass, polymer beads, or a metal oxide. Embodiment 16 is the photocatalyst of any one of embodiments 1 to 15, wherein the photocatalyst is capable of catalyzing the photocatalytic electrolysis of water. Embodiment 17 is the photocatalyst of any one of embodiments 1 to 16, wherein the photocatalyst is included in a composition that includes water. Embodiment 18 is the photocatalyst of embodiment 17, wherein the composition further includes a sacrificial agent. Embodiment 19 is the photocatalyst of embodiment 18, wherein the sacrificial agent is methanol, ethanol, propanol, iso-propanol, n-butanol, iso-butanol, ethylene glycol, propylene glycol, glycerol, oxalic acid, trimethyl amine, triethanolamine, or any combination thereof. Embodiment 20, is the photocatalyst of embodiment 19, wherein the sacrificial agent is ethanol. Embodiment 21 is the photocatalyst of any one of embodiments 18 to 20, wherein the composition includes a sacrificial agent to water volume ratio of less than 20:80, preferably from 1:99 to 15:85, or more preferably from 1:99 to 10:90. Embodiment 22 is the photocatalyst of embodiment 21, wherein the $H_2$ production rate from water is 2 to 12 mmol/$g_{Catal}$ hour, preferably 5 to 12 mmol/$g_{Catal}$ hour, and most preferably from 10 to 12 mmol/$g_{Catal}$ hour using a light source having a flux from about 0.1 to 10 mW/$cm^2$ at 360 nm.

**[0013]** Embodiment 23 is a system for producing hydrogen gas and oxygen gas from water, the system includes (a) a transparent container including a composition that includes the photocatalyst of any one of embodiments 1 to 22, water, and a sacrificial agent; and (b) a light source for irradiating the composition. Embodiment 24 is the system of embodiment 23, wherein the light source is sunlight. Embodiment 25 is the system of embodiment 24, wherein the light source is an ultra-violet or an ultra-violet/visible lamp.

**[0014]** Embodiment 26 is a method for producing hydrogen gas and oxygen gas from water, the method includes obtaining a system of any one of embodiments 23 to 25 and subjecting the composition to the light source for a sufficient period of time to produce hydrogen gas and oxygen gas from the water.

**[0015]** Embodiment 27 is a method of making any one of the photocatalysts of embodiments 1 to 22, the method includes (a) obtaining a titanium dioxide support material having a Ni(II) complex dispersed on the support material; and (b) heating the titanium dioxide support material and reducing the Ni(II) to Ni(0) with a gas that includes $H_2$ to form the photocatalyst. Embodiment 28 is the method of embodiment 27, wherein the Ni(II) in step b is NiO. Embodiment 29 is the method of any one of embodiments 27 to 28, wherein the gas further includes $N_2$. Embodiment 30 is the method of any one of embodiments 27 to 29, wherein the titanium dioxide support material is heated at a temperature of 350 $^{o}$C to 700 $^{o}$C for at least one hour. Embodiments 31 is the method of embodiment 30, wherein the titanium dioxide support material is heated at a temperature of 450 $^{o}$C to 550 $^{o}$C for 1 to 3 hours or for 2 hours. Embodiment 32 is the method of any one of embodiments 27 to 31, wherein obtaining the titanium dioxide support material includes forming the Ni(II) complex on the support material. Embodiment 33 is the method of embodiment 32, wherein forming the Ni(II) complex on the support material includes (i) combining a nickel (II) salt and glycerol with water to form an aqueous solution of a Ni(II)-glycerol complex; (ii)adding titanium dioxide support material to the solution; (iii) precipitating the Ni(II)-glycerol complex on the titanium dioxide support material with a basic media to form a mixture; (iv) agitating the mixture; (v) removing all or substantially all the liquids from the mixture and collecting the solids; (vi) washing the solids with water; and (vii) drying and calcining the solids. Embodiment 34 is the method of embodiment 33, wherein the step of precipitating the Ni(II)-glycerol complex on the $TiO_2$ support material by the addition of basic media includess dropwise addition of an aqueous solution of NaOH with stirring. Embodiment 35 is the method of embodiment 34, wherein said addition and stirring is performed until the mixture attains a pH of about 12. Embodiment 36 is the method of any one of embodiments 33 to 35, wherein said step of agitating the resulting mixture includes stirring for an additional period of one hour. Embodiment 37 is the method of any one of embodiments 33 to 36, wherein said step of removing all or substantially all the liquids from the mixture and collecting the solids includes vacuum filtration. Embodiment 38 is the method of embodiment 37, wherein the solids include $Ni(OH)_2/TiO_2$. Embodiment 39 is the method of

any one of embodiments 33 to 38, wherein said calcining includes heating at a temperature of 300 $^{o}$C for two hours. Embodiment 40 is the method of claim 39, wherein calcining forms NiO.

**[0016]** The following includes definitions of various terms and phrases used throughout this specification.

**[0017]** "Water splitting" or any variation of this phrase describes the chemical reaction in which water is separated into oxygen and hydrogen.

**[0018]** "Average particle size of less than or equal to 1 nm" refers to particles of semi-spherical Ni metal with a total number of 500 atoms or less in contact with the $TiO_2$ support.

**[0019]** "Nanoparticle" refers to particles having a mean particle size of less than 100 nanometers.

**[0020]** "Microparticle" refers to particles having a mean particle size of 100 nm or more.

**[0021]** "Inhibiting," "preventing," or "reducing" or any variation of these terms, when used in the claims or the specification includes any measurable decrease or complete inhibition to achieve a desired result. By way of example, reducing the likelihood for an excited electron in the conductive band to recombine with a hole in the valence band encompasses situations where a decrease in the number of electron/hole recombination events occurs or an increase in the time it takes for an electron/hole recombination event to occur such that the increase in time allows for the electron to reduce hydrogen ions rather than to recombine with its corresponding hole. In either instance, the photocatalysts of the present invention can be compared with photocatalysts of other transition metal $TiO_2$ photocatalyst or noble metal catalysts.

**[0022]** "Effective" or any variation of this term, when used in the claims or specification, means adequate to accomplish a desired, expected, or intended result.

**[0023]** The terms "about" or "approximately" are defined as being close to as understood by one of ordinary skill in the art, and in one non-limiting embodiment the terms are defined to be within 10%, preferably within 5%, more preferably within 1%, and most preferably within 0.5%.

**[0024]** The use of the word "a" or "an" when used in conjunction with the term "comprising" in the claims or the specification may mean "one," but it is also consistent with the meaning of "one or more," "at least one," and "one or more than one."

**[0025]** The words "comprising" (and any form of comprising, such as "comprise" and "comprises"), "having" (and any form of having, such as "have" and "has"), "including" (and any form of including, such as "includes" and "include") or "containing" (and any form of containing, such as "contains" and "contain") are inclusive or open-ended and do not exclude additional, unrecited elements or method steps.

**[0026]** The photocatalysts of the present invention can "comprise," "consist essentially of," or "consist of" particular components, compositions, ingredients, etc. disclosed throughout the specification. With respect to the transitional phase "consisting essentially of," in one non-limiting aspect, a basic and novel characteristic of the photoactive catalysts and materials of the present invention are their ability to efficiently use excited electrons in water-splitting applications to produce hydrogen.

**[0027]** The terms "wt.%" or "vol.%" refers to a weight or volume percentage of a component based on the total weight or volume of material that includes the component. In a non-limiting example, 10 grams of metal in 100 grams of the catalyst is 10 wt.% of metal.

**[0028]** Other objects, features and advantages of the present invention will become apparent from the following figures, detailed description, and examples. It should be understood, however, that the figures, detailed description, and examples, while indicating specific embodiments of the invention, are given by way of illustration only and are not meant to be limiting. Additionally, it is contemplated that changes and modifications within the spirit and scope of the invention will become apparent to those skilled in the art from this detailed description.

## BRIEF DESCRIPTION OF THE DRAWINGS

**[0029]** **FIG. 1** is a schematic illustration of important electron transfer processes using the photocatalyst of the present invention..

**[0030]** **FIG. 2** is a schematic of an embodiment of a water-splitting system using the photocatalysts of the invention.

**[0031]** **FIG. 2A** is an expanded view of photocatalyst in the water-splitting system of FIG. 2.

**[0032]** **FIG. 3A** is an image of $NiO/O_2$ photocatalyst precursors.

**[0033]** **FIG. 3B** is an image and $Ni/TiO_2$ photocatalysts obtained by $H_2$ reduction of the $NiO/TiO_2$ samples in FIG. 3A.

**[0034]** **FIG. 4A** are UV-Visible absorbance spectra for the photocatalyst precursors of the present invention.

**[0035]** **FIG. 4B** are Tauc plots for the photocatalysts precursors of the present invention.

**[0036]** **FIG. 5A** are UV-Visible absorbance spectra for the photocatalyst of the present invention.

**[0037]** **FIG. 5B** are Tauc plots for the photocatalysts of the present invention.

**[0038]** **FIG. 6** are TGA curves for photocatalysts of the present invention in air collected at a heating rate of 10 $^{o}C\ min^{-1}$.

**[0039]** **FIG. 7** is a TEM images for a photocatalyst of the present invention having 4 wt.% nickel; and (d) 2 wt.% $Au/TiO_2$.

**[0040]** **FIG. 8** is a TEM images for a comparative 2 wt.% $Au/TiO_2$ photocatalyst.

**[0041]** **FIG. 9** are powder X-ray Diffraction (XRD) patterns for photocatalyst precursors of the present invention, support material, metallic nickel powder, and nickel oxide.

**[0042]** **FIG. 10** are powder XRD patterns for photocatalyst of the present invention, support material, metallic nickel powder, and nickel oxide.

**[0043]** **FIG. 11** are Ni 2p XPS spectra for photocatalyst precursors of the present invention, photocatalysts of the present invention, metallic nickel powder, and $NiTiO_3$.

**[0044]** **FIG. 12** are Ni 2p XPS spectra for the support material, photocatalyst precursors of the present invention, and photocatalysts of the present invention.

**[0045]** **FIG. 13** are Ni L-edge NEXAFS spectra for photocatalyst precursors of the present invention, photocatalyst of the present invention, metallic nickel powder, and nickel oxide.

**[0046]** **FIG. 14** are photoluminescence spectra of the support material, and the photocatalyst precursors of the present invention. The insets show plots of normalized photoluminescence intensity versus NiO.

**[0047]** **FIG. 15** are photoluminescence spectra for the support material and photocatalysts of the present invention. The insets show plots of normalized photoluminescence intensity versus Ni loading.

**[0048]** **FIG. 16** are plots of $H_2$ production versus time for photocatalysts of the present invention and a comparative Au/P25 $TiO_2$ photocatalyst in an ethanol:water mixture (80:20 by volume) under UV irradiation.

**[0049]** **FIG. 17** are plots of $H_2$ production versus time for a photocatalyst precursor of the present invention and a photocatalyst of the present invention in an ethanol:water mixture (80:20 by volume) under UV irradiation.

**[0050]** **FIG. 18** are plots of rates of $H_2$ production versus Ni loading in 10 vol.% and 80 vol.% aqueous ethanol solutions for photocatalysts of the present invention.

**[0051]** **FIG. 19** are plots of $H_2$ production rates versus inverse normalized photoluminescence intensities from photocatalyst 0.5 wt.% Ni/$TiO_2$ from FIG. 13 at volume ratios of ethanol to water of 10:90 and 80:20.

**[0052]** **FIG. 20** are plots of rates of $H_2$ production versus ethanol concentration for two photocatalysts of the present invention and a comparative 2 wt.% Au/P25 $TiO_2$ photocatalyst under UV irradiation.

## DETAILED DESCRIPTION OF THE INVENTION

**[0053]** While hydrogen-based energy from water has been proposed as a solution to the current problems associated with carbon-based energy (e.g., limited amounts and fossil fuel emissions), the currently available technologies are expensive, inefficient, and/or unstable. The present application provides a low cost and effective solution to these issues. The solution is predicated on the use of a transition metal titanium dioxide photocatalyst. Specifically, the photocatalyst includes $Ni^0$ metal particles having an average particle size of less than or equal to 1 nm or less than 1 nm dispersed on the surface of a titanium dioxide support. It has been unexpectedly found that photocatalyst of the invention produces higher amounts of hydrogen in photocatalytic water-splitting reactions than noble metal titanium dioxide photocatalysts at low ethanol to water ratios (e.g., less than 10:90 or 5:95 See, for example, Example 3). FIG. 1 is schematic of photocatalytic hydrogen production in the system of the present invention using an ethanol water mixture. Upon UV excitation, electrons are promoted from the valence band of $TiO_2$ into the conduction band, generating the electron-hole pairs. Holes in the valence band (VB) migrate to the $TiO_2$ surface and oxidize ethanol, acetaldehyde and water to generate $H^+$ while electrons in the conduction band (CB) of $TiO_2$ reduce any surface Ni (II) to $Ni^0$ ($Ni^{+2}$ to $N^0$, -0.23 V) or migrate onto pre-

existing $Ni^0$ particles which act as cathodic sites for $H_2$ evolution as shown in the reaction (I) below:

$$2H^+ + 2e^- \rightarrow H_2 \quad (I).$$

**[0054]** Without wishing to be bound by theory, it is believed that his increase can be attributed to ethanol oxidation to acetaldehyde at the $TiO_2$ surface as in the reaction (II) below:

$$C_2H_5OH + 2h^+ \rightarrow CH_3CHO + 2H^+ \quad (II)$$

and the subsequent oxidation of acetaldehyde to acetic acid as shown in the reaction (III) below:

$$CH_3CHO + 2h^+ + H_2O \rightarrow CH_3COOH + 2H^+ \quad (III)$$

These processes are mediated by photoexcited holes migrating to the $TiO_2$ surface, and are energetically favourable processes compared to the splitting of water to oxygen and $H^+$ as shown in the reaction (IV) below and thus occur at a faster rate.

$$H_2O + 2H^+ \rightarrow \tfrac{1}{2}O_2 + 2H^+ \quad (IV)$$

**[0055]** Thus the maximum $H_2$ production rate of the photocatalysts at high ethanol concentrations, before dropping sharply in the absence of ethanol can be attributed to the oxidation of acetaldehyde to acetic acid. It was also surprisingly found that an inverse relationship was observed between the photoluminescence behaviour and the photo-catalytic activity when the water-splitting was performed in the presence of a sacrificial agent (See, FIG. 19). This inverse relationship is believed to be due to the competing processes (electron – hole recombination "radiative recombination" and charge transfer "hydrogen ions reduction") occurring during the water-splitting process.

**[0056]** These and other non-limiting aspects of the present invention are discussed in further detail in the following sections.

## A. Photoactive Catalysts

**[0057]** The photocatalyst is composed of nickel(0) particles having an average particle size of less than or equal to 1 nm, preferably less than 1 nm, dispersed on a titanium dioxide support. The photocatalyst can have a Brunauer-Emmett-Teller (BET) surface area of 43, 44, 45 or 46 $m^2g^{-1}$ and/or a Ni(0) to Ti atom% of greater than 0 to 0.07, 0.01, 0.02, 0.03 or 0.04 or any value there between The photocatalyst can have a Ni(0) content from greater than 0 to

4 wt.% or 0.1 to 4 wt. %, 0.2 to 2 wt. %, 0.3 to 1 wt.%, 0.4 to 0.8 wt.%, 0.4 to 0.6 wt. % or 0.1, 0.2, 0.3, 0.4, 0.5, 0.6, 0.7. 0.8, 0.9, 1 wt.%, or any value there between. In one particular aspect, the photocatalyst does not include any one of gold, ruthenium, rhenium, rhodium, palladium, silver, copper, osmium, iridium, and platinum. The photocatalyst can, in some instances, consist essentially of nickel and titanium dioxide. The Ni(0) can be obtained, *in situ*, from hydrogen reduction of a photocatalyst precursor $NiO/TiO_2$. In some embodiments, the photocatalyst includes a mixture of Ni(0) and NiO. NiO is not considered detrimental to the photocatalyst as NiO can also catalyze the water-splitting, albeit at a slower rate (the Ni(II) must first oxidize to Ni(0)). The photocatalyst precursor can be treated in the presence of a reducing agent (e.g., hydrogen gas) to reduce the Ni(II) to metallic nickel (Ni(0)). Without wishing to be bound by theory it is believed that *in situ* reduction of the Ni(II) provides sub-micron particles of Ni(0) on the surface of the titanium dioxide support.

### 1. Titanium Dioxide Support

**[0058]** The titanium dioxide support can be particles, particles ground into a powder, or both. The titanium dioxide particles can have two main polymorphs, anatase and rutile. In some embodiments, the titanium dioxide particles can include brookite. In a preferred aspect, the particles include anatase and rutile phases. The $TiO_2$ support can have a ratio of anatase and rutile phase ranges from 1.5:1 to 10:1, from 6:1 to 5:1, or from 5:1 to 4:1. The percentage of anatase to rutile the titanium dioxide polymorph can be determined using powder X-ray diffraction (XRD) techniques. For example, a Philips X'pert-MPD X-ray powder diffractometer may be used to analyze powder samples of titanium dioxide polymorphs. Using the areas of these peaks the amounts of rutile phase in the titanium dioxide polymorph can be determined using the following equation:

$$\%\, rutile = \frac{1}{\left(\frac{A}{R}\, x\, 0.884\right)+1} \times 100 \qquad (1)$$

where A is the area of anatase peak; R is the area of rutile peak as determined by XRD; and 0.884 is a scattering coefficient.

**[0059]** In some embodiments, the anatase to rutile phases in the titanium dioxide particles can be formed by heat treating single phase anatase to transform some of the anatase phase into a rutile phase. For example, titanium dioxide anatase particles can be heated to a temperature of 780 °C to obtain mixed phase titanium dioxide particles. In other embodiments, titanium dioxide rutile phase particles can be mixed with titanium dioxide anatase particles to obtain the desired ratio. The mean particle size of the mixed phase or

single phase $TiO_2$ nanoparticles is less than 100 nm. The $TiO_2$ nanoparticles have a mean particle size of less than 95 nm, from about 10 nm to about 80 nm, from about 15 nm to about 50 nm, from about 20 nm to about 50 nm, or from about 15 nm to about 20 nm, or 10 nm, 20 nm, 30 nm, 40 nm, 50 nm, 60 nm, 70 nm, 80 nm, 90 nm, 91 nm, 92 nm, 93 nm, 94, or any value or range there between. A BET surface area of the $TiO_2$ nanoparticles can range from 40 to 60 $m^2/g$ or any value or range there between. Titanium dioxide nanoparticles are commercially available as Aeroxide® P25 from Evonik Industries (Germany) or as titanium (IV) oxide powder from Sigma-Aldrich® (USA).

### 2. Active Metals

**[0060]** Ni(0) metal is obtained through heating and, *in situ*, reduction of a Ni(II) species using hydrogen under inert conditions. The Ni(II) species can be a nickel (II) oxide obtained from thermal decomposition of a nickel hydroxide on the titanium dioxide surface.

### 3. Preparation of Photoactive Material

**[0061]** The photocatalyst can be prepared using known metal-complex precipitations method. A non-limiting example of metal-complex precipitation method is described by Yoong *et al.* in *Energy*, 34 (2009) 1652-1661. In a non-limiting example, nickel nitrate hexahydrate can be a dissolved in ultra-pure water and a complexing agent can be added to generate a Ni(II)-complexing agent complex. Non-limiting examples of complexing agents include organic short chain alcohols such as glycerol. A molar ratio of Ni(II) to complexing agent can be 1:2. The titanium dioxide support can be added to the aqueous solution of nickel-glycerine complex with continuous stirring to form a suspension. Addition of base (e.g., sodium hydroxide) dropwise into the mixture under constant stirring precipitates the nickel-hydroxide $Ni(OH)_2$ on the titanium dioxide support. Base can be added with stirring until a pH of 11 to 13, or 11, 11.5, 12, 12.5, 13, or any range or value there between is reached. In one aspect, a pH of 12 is reached. The precipitate ($Ni(OH)_2/TiO_2$) can be stirred further at an elevated rate of agitation for a desired amount of time (e.g., 0.5 h, 1 h, 1.5 h, or 2 h). The precipitate can be separated from the basic solution using known filtration techniques and washed one or more times with water, preferably ultra-pure water, to remove any residual base. The washed precipitate is green in color and includes $Ni(OH)_2/TiO_2$. The washed precipitate can be dried under atmospheric conditions (e.g., in air) at a temperature of about 60 °C to 100 °C, 65 °C to 90 °C, or 70 °C to 75 °C. The $Ni(OH)_2/TiO_2$ precipitate can be converted to $NiO/TiO_2$ by calcining the precipitate at 300 °C, 400 °C or 500 °C for a desired

period of time (e.g., 0.5 h, 1 h, or 1.5 h) in the presence of an oxygen source (e.g., air). The $NiO/TiO_2$ photocatalyst precursor can be heated under a flow of hydrogen containing gas until the $NiO/TiO_2$ is fully or substantially converted to $Ni/TiO_2$ (e.g. for 1 h, 2 h or 3 h). Heating temperatures can range from 300 °C, 400 °C or 500 °C. The hydrogen containing gas can be hydrogen gas or a mixture of hydrogen gas and inert gases (e.g., $H_2$ and $N_2$). The flow of the hydrogen containing gas can be 50 mL/min, 100 mL/min 150 mL/min and can be adjusted such that a suitable amount of hydrogen contacts the $NiO/TiO_2$ photocatalyst precursor.

## B. Water-Splitting System

**[0062]** FIG. 2 is a schematic of an embodiment of water-splitting system 100. Water-splitting system 200 includes container 202, photocatalyst 204, light source 206, and water 208. Container 202 can be translucent or even opaque such as those that can magnify light (e.g., opaque container having a pinhole(s)). Photocatalyst 204 includes nickel(0) particles of less than or equal to 1 nm, preferably less than 1 nm, on a titanium dioxide support ($Ni/TiO_2$) and is shown as single nanoparticles dispersed in the media. Light source 206 is sunlight, a UV lamp, or an Infrared (IR) lamp. An example of a UV light is a 100 Watt ultraviolet lamp with a flux of about 2 $mW/cm^2$ at a distance of 10 cm. The UV lamp can be used with a 360 nm and above filter. Such UV lamps are commercial available from, for example, Sylvania. Photocatalyst 204 can be used to split water to produce $H_2$ and $O_2$ as shown in FIG. 2A, which is an exploded view of the region near a photocatalyst 204 in water-splitting system 204. Light source 206 contacts photocatalyst 204, thereby exciting electrons (e-) from their valence band to their conductive band, thereby leaving corresponding holes (h+). Referring back to FIG. 1, the holes in the valence band (VB) migrate to the $TiO_2$ surface and oxidize ethanol, acetaldehyde and water, to generate $H^+$ while electrons in the conduction band (CB) of $TiO_2$ reduce any surface Ni (II) to $Ni^0$ ($Ni^{+2}$ to $N^0$ is -0.23 V) or migrate onto pre-existing $Ni^0$ clusters which act as cathodic sites for $H_2$ evolution ($2H^+ + 2e^- \rightarrow H_2$). Due to electroconductive material (e.g., Ni(0)) deposited on the surface of titanium dioxide support, the excited electrons are more likely to be used to split water before recombining with holes than would otherwise be the case. Notably, system 200 does not require the use of an external bias or voltage source. Further, the efficiency of system 200 allows for one to avoid or use minimal amounts of a sacrificial agent. In some embodiments, the photocatalyst is supported on (e.g., adhered or coupled to) a substrate such as glass, polymer beads, or a metal oxide.

**[0063]** In addition to being capable of catalyzing water splitting without an external bias or voltage, the photocatalysts of the present invention may be included in an anode of an electrochemical cell capable of forming oxygen and hydrogen by electrolysis of water. In a non-limiting example, light energy may be provided to a photocell and from the light energy a voltage between the anode and the cathode is produced and water molecules are split to form hydrogen and oxygen. The method can be practiced such that the hydrogen production rate from water can be modified as desired by subjecting the system to various amounts of light or light flux.

## EXAMPLES

**[0064]** The present invention will be described in greater detail by way of specific examples. The following examples are offered for illustrative purposes only, and are not intended to limit the invention in any manner. Those of skill in the art will readily recognize a variety of noncritical parameters which can be changed or modified to yield essentially the same results.

### Example 1
### (Photocatalyst Preparation)

**[0065]** **Materials**. Nickel(II) nitrate hexahydrate (≥97%), glycerol (≥99%), urea (≥99.5%), sodium hydroxide (≥98%), Evonik P25 $TiO_2$, absolute ethanol (≥99.5%) and NiO (≥99.9%) were all obtained from Sigma-Aldrich and used without further purification. All solutions were prepared using milli-Q water (18.2 MΩ·cm resistivity). A reference photocatalyst, 2 wt.% $Au/TiO_2$, was prepared using the deposition-precipitation with urea method described by Zanella et al. in *J. Phys. Chem. B*, 106 (2002) 7634-7642. A further reference sample, $NiTiO_3$, was prepared according to Salvador *et al.* in *Appl. Phys. Lett.*, 40 (1982) 188-190.

**[0066]** **Synthesis of Ni(0)$TiO_2$ nanoparticle samples.** A series of $NiO/TiO_2$ samples with nominal NiO loadings of 0-5 wt.% listed in Table 1 were prepared. Nickel (II) nitrate hexahydrate and glycerol (1:2 molar ratio) were added to ultrapure water of type 1 (200 mL, Milli-Q®, Millipore Corporation, USA) to form an aqueous nickel(II)-glycerol complex. The exact masses of nickel (II) nitrate hexahydrate and glycerol used depended on the target nominal NiO loading. The target nominal Ni loading is shown in Table 1. The P25 $TiO_2$ (10 g) was added to the solution containing the nickel(II)-glycerol complex with continuous stirring. The nickel-glycerol complex was then precipitated on the $TiO_2$ support by the drop wise addition of 0.5 M NaOH under constant stirring until a pH of 12 was reached. The

resulting suspension was stirred for a further 1 h, then the resulting light green powders ($Ni(OH)_2/TiO_2$) were collected by vacuum filtration. After washing repeatedly with ultrapure water, the $Ni(OH)_2/TiO_2$ powders were dried overnight at 70 °C in air. $NiO/TiO_2$ photocatalysts were obtained by calcination of the $Ni(OH)_2/TiO_2$ powders at 300 °C for 2 h.

**[0067]** The $Ni/TiO_2$ photocatalysts (0-4 wt.% nominal loadings, Table 1, Samples 12-19) were obtained by heating the 0-5 wt.% $NiO/TiO_2$ photocatalysts (Samples 2-9, respectively) under a $H_2/N_2$ flow (10 vol.% $H_2$, 100 mL $min^{-1}$) at 500 °C for 2 h. This treatment reduced adsorbed Ni(II) species to metallic form as evidence by a change of the powders from green (characteristic of NiO) to grey (characteristic of finely dispersed $Ni^0$). FIGS. 3A and 3B are images of $TiO_2$ support (Sample 1) and photocatalyst precursor material ($NiO/TiO_2$ Samples 2-9) before and the photocatalyst of the present invention ($Ni/TiO_2$, Samples 12-19). FIG. 3A is an image of bottles containing the photocatalyst precursor materials for Samples 2 and 4-9 and titanium dioxide (Sample 1). All the photocatalyst precursor materials (Samples 2 and 4-9) were light green, which is characteristic for NiO. FIG. 3B is an image of bottles containing the photocatalyst material (Samples 12 and 14-19), and $H_2$ treated $TiO_2$ (Sample 10). As shown in FIG. 3B all the photocatalyst (Samples 12 and 14-19) were light grey to very dark grey depending on the metal loading. Physico-chemical characterisation studies and photocatalytic tests were subsequently conducted on both the $NiO/TiO_2$ and $Ni/TiO_2$ photocatalysts are described below in Example 2. Table 2 lists physical, chemical and optical data for Samples photocatalysts. Relevant data for a number of reference materials is also provided.

**Table 1**

| Sample No. | Description |
|---|---|
| 1 | P-25 $TiO_2$ |
| 2 | 0.16 wt.% $NiO/TiO_2$ |
| 3 | 0.31 wt.% $NiO/TiO_2$ |
| 4 | 0.47 wt.% $NiO/TiO_2$ |
| 5 | 0.63 wt.% $NiO/TiO_2$ |
| 6 | 0.9 wt.% $NiO/TiO_2$ |
| 7 | 1.25 wt.% $NiO/TiO_2$ |
| 8 | 2.5 wt.% $NiO/TiO_2$ |
| 9 | 5.0 wt.% $NiO/TiO_2$ |
| 10 | NiO |
| 11 | P-25 $TiO_2$ after $H_2$ treatment |
| 12 | 0.13 wt.% $Ni/TiO_2$ |
| 13 | 0.25 wt.% $NiTiO_2$ |
| 14 | 0.38 wt.% $Ni/TiO_2$ |
| 15 | 0.5 wt.% $Ni/TiO_2$ |
| 16 | 0.75 wt.% $Ni/TiO_2$ |
| 17 | 1.0 wt.% $Ni/TiO_2$ |
| 18 | 2 wt.% $Ni/TiO_2$ |
| 19 | 4 wt.% $Ni/TiO_2$ |
| 20 | Metallic Ni |
| 21 | $NiTiO_3$ |

## Example 2
## (Photocatalyst Precursor and Photocatalyst Characterization)

### A. UV-Visible Absorbance

**[0068]** UV-visible absorbance spectra were recorded over the range 250-900 nm on a Shimadzu UV-2101 PC spectrophotometer equipped with an ISR-240A integrating sphere attachment. Barium sulfate was used as a reflectance standard.

**[0069]** **Photocatalyst Precursor** FIG. 4A are UV-Visible spectra of the support material (P-25 $TiO_2$, Sample 1, data line S1) photocatalyst precursor material (Samples 2, 3 and 5-9, data lines S2, S3 and S5 through S9) and nickel oxide (Sample 10, data line S10). FIG. 4B are corresponding Tauc plots of the support material (Sample 1, data line S1) and the

photocatalyst precursor (Samples 2, 3, and 5, 6, 8, and 9, data lines S2, S3, S5, S6, S8, and S9). Referring to FIG. 4A, the intense absorption below 400 nm was attributed to the $TiO_2$ support ($E_g$ = 3.15 eV). The samples also showed additional absorption features at visible and near IR wavelengths which intensified on increasing the nominal NiO loading, which were assigned to NiO on the $TiO_2$ support based on reference spectra. NiO shows many absorption peaks in the visible region due to d-d transitions involving octahedral coordinated $Ni^{2+}$ ions and which are responsible for the characteristic light-green color of NiO.

**[0070] Photocatalyst.** FIG. 5A are UV-visible spectra of the support material (Sample 1, data line S1) and the photocatalyst of the present invention (Samples 12, 13, and 15-19, data lines S12, S13, and S15 through S19). FIG. 5B are corresponding Tauc plots of the support material (Sample 1, data line S1) and the photocatalyst precursor (Samples 12, 13, and 15-19, data lines S12, S13, and S15 through S19, respectively). The intense absorption below 400 nm was attributed to the $TiO_2$ support. Referring to FIG. 5A, the strong absorption across the entire visible spectrum is seen for the $Ni/TiO_2$ photocatalysts, which is not as strong in the photocatalyst precursor spectra (FIG. 4A). A strong absorption was deemed consistent with metallic Ni formation, and was confirmed by TGA and X-ray technique analyses below. In all of the spectra, the intensity of the Ni related absorption signals increased linearly with nominal Ni loading. Band gap energies for the different $Ni/TiO_2$ photocatalysts are summarised in Table 1.

## B. Thermogravimetric (TGA)

**[0071]** Thermogravimetric (TGA) analyses were performed on a Shimadzu TGA-50 thermogravimetric analyser. Selected photocatalysts were heated in air from room temperature to 800 to 1000 °C at a heating rate of 10 °C $min^{-1}$.

**[0072] Photocatalyst.** FIG. 6 are TGA curves for photocatalysts (Samples 17-19, data lines 604, 606 and 608) and the support material (Sample 1, data line 602) with heating in air from room temperature to 800 °C. All samples showed a 1-2 % mass loss below 200 °C due to desorption of surface chemisorbed water. Above 400 °C, the support material (Sample 1) and the photocatalysts (Samples 17-19) had mass gains of 0, 0.3, 0.6 and 1.1%, respectively, which was attributed to the oxidation of the supported $Ni^0$ to NiO. The experimental mass gains were in near perfect accord with the theoretical mass gains expected for the conversion of $Ni/TiO_2$ to $NiO/TiO_2$ (0, 0.27, 0.53 and 1.04 %, respectively). TGA data for a 5 wt.% $NiO/TiO_2$ photocatalyst (not shown) displayed negligible mass gain above 400 °C,

confirming that the oxidation of NiO to $Ni_2O_3$ did not occur over the temperature range of the TGA experiments.

### C. Transmission Electron Microscopy (TEM)

**[0073]** TEM images were collected using a TECNAI 12 transmission electron microscope. Powder samples were dispersed in absolute ethanol and then 3 μL of the resulting dispersion placed on carbon coated copper TEM grids for analysis.

**[0074]** FIG. 7 is a TEM image of the photocatalyst of the invention (Sample 19, 4 wt% $Ni/TiO_2$). The nickel(0) nanoparticles could not be identified with any certainty. Thus, it was concluded that the Ni nanoparticles are < 1 nm in size and at the resolution limit of the TEM instrument, and that any Ni present was highly dispersed over the $TiO_2$ support (likely as sub nanometer sized particles or even subsurface Ni particles), which is believed, without being bound by theory, that a very strong metal-support interaction between $Ni^0$ and $TiO_2$ existed. In comparison, FIG. 8 is a TEM analysis of 2 wt.% $Au/TiO_2$ photocatalyst showing Au nanoparticles of average size ~ 5 nm, which were easily discernible from the $TiO_2$ support.

### D. X-Ray Diffraction (XRD)

**[0075]** Powder XRD patterns were taken on a Siemens D5000 Diffractometer equipped with a Cu anode X-ray tube and a curved graphite filter monochromator. XRD data was collected from $2\theta$ = 10-90° (step 0.02°, scan rate $2^o$ $min^{-1}$) using Cu Kα X-rays ($\lambda$ = 1.5418 Å, 40 mA, 40 kV). Anatase and rutile crystallite sizes (L) were determined from the powder XRD data using the Scherrer equation and line-widths of the anatase (101) reflection at $2\theta$ = $25.3^o$ and rutile (110) reflection at $2\theta$ = $27.4^o$, respectively. The rutile:anatase ratio in the samples was determined according to the method described by Ding *et al.* in *J. Mater. Sci. Lett.*, 15 (1996) 1789-1791.

$$\%Rutile = \frac{1}{[1 + 0.8(I_A / I_R)]} \times 100$$

where $I_A$ is the peak intensity for the anatase (101) reflection, and

$I_R$ is the peak intensity for the rutile (110) reflection.

**[0076]** **Photocatalyst Precursor.** FIG. 9 are XRD patterns for the TiO2 support material (Sample 1, pattern 902), photocatalyst precursor material ($NiO/TiO_2$) (Samples 2, 3, 5, and 7-9, patterns 904, 906, 908, 910, 912, 914, 916 respectively), metallic nickel powder (Sample

21, pattern 918) and nickel oxide (Sample 10, pattern 920). No NiO related features were seen in the XRD patterns of data patterns 904-916, indicating that the supported NiO phase was likely either amorphous or incorporated into the $TiO_2$ lattice.

**[0077] Photocatalyst.** FIG. 10 are powder XRD patterns for the support material (Sample 1, pattern 1002), the photocatalysts of the present invention (Samples 12-14 and 16-19, patterns 1004, 1006, 1008, 1010, 1012, 1014 and 1016 respectively), metallic nickel (Sample 21, pattern 1018) and nickel oxide (Sample 10, pattern 1020) over the 2θ range 40-60°. The XRD patterns for all the $Ni/TiO_2$ photocatalysts were dominated by peaks due to anatase and rutile in the P25 $TiO_2$ support. From the relative intensity of the anatase (101) and rutile (110) reflections, the anatase:rutile weight ratio in the P25 $TiO_2$ support was estimated to be 6:1. Average anatase and rutile particle sizes, estimated from the FWHM of the anatase (101) and rutile (110) reflections using the Scherrer equation, were 25 nm and 50 nm, respectively. For the photocatalysts of the present invention (Samples 17-19) weak and broad peaks due to metallic *f.c.c.* Ni are seen at Ni loadings > 1 wt.%, which intensify linearly with the nominal Ni loading.

## E. X-ray Photoelectron Spectroscopy (XPS)

**[0078]** XPS data was collected using a Kratos Axis UltraDLD equipped with a hemispherical electron energy analyser and an analysis chamber of base pressure $\sim 1 \times 10^{-9}$ Torr. Spectra were excited using monochromatic Al Kα X-rays (1486.69 eV), with the X-ray source operating at 150 W. Samples were gently pressed into thin pellets of ~0.1 mm thickness for the analyses. A charge neutralisation system was used to alleviate sample charge build up during analysis. Survey scans were collected at a pass energy of 80 eV over the binding energy range 1200-0 eV, while core level scans were collected with a pass energy of 20 eV. The spectra were calibrated against the C 1s signal at 285.0 eV from adventitious hydrocarbons. Ni L-edge NEXAFS data was collected on the soft X-ray Beamline at the Australian Synchrotron. NEXAFS data was taken in the partial electron yield (PEY) mode at an analysis chamber pressure of $\sim 1 \times 10^{-10}$ Torr. The PEY data was normalized against a current measured simultaneously on a gold mesh in the beam line to eliminate potential spectral artifacts caused by fluctuations in the beam intensity while scanning. The measurements were carried out in high resolution (HR) mode by increasing the photon energies in steps of 0.05 or 0.1 eV. Elements identified in XPS survey spectra of the photocatalysts (not shown) were Ni, Ti, O and C with the latter being due primarily to adventitious hydrocarbons. Quantitative XPS analyses were performed using peak areas of

the Ni 2p, Ti 2p, O 1s and C 1s signals, results for which are presented in Table 1. The Ni:Ti ratio in the $Ni/TiO_2$ samples increased with the nominal Ni loading, though not linearly (Table 1). The O:Ti ratio for all the $NiO/TiO_2$ and $Ni/TiO_2$ samples was ~2, as expected for $TiO_2$-based photocatalysts.

**[0079] Photocatalyst Precursor.** XPS was used to probe the near surface region chemical composition and the valence state of nickel in the $NiO/TiO_2$ and $Ni/TiO_2$ photocatalysts. FIG. 11 are Ni 2 p XPS spectra for the photocatalyst precursor, the photocatalyst, and reference materials. Spectra 1102 is a Ni 2 p XPS spectra for the photocatalyst precursor (Sample 9). Spectra 1106 is a Ni 2 p XPS spectra metallic nickel. Spectra 1108 is a Ni 2 p XPS spectra of nickel oxide. Spectra 1110 is a Ni 2 p XPS spectra of nickel titanate ($NiTiO_3$). The Ni 2p XPS spectrum for the photocatalyst precursor (Sample 9, spectra 1102) showed peaks at 855.6 eV and 873.2 eV, in a 2:1 area peak area ratio, which are assigned to the Ni $2p_{1/2}$ and Ni $2p_{3/2}$ signals, respectively, of a Ni(II) species on $TiO_2$. Comparing spectra 1102 to spectra 1108, the samples are similar except that spectra 1102 lacked the multiplet fine structure seen for the NiO. Comparing spectra 1102 to spectra 1110, it was observed that spectra 1102, and thus Sample 9 is similar to nickel titanate. However, $NiTiO_3$ was not expected to form under the conditions used to synthesize the $NiO/TiO_2$ photocatalysts, thus spectra 1102 was interpreted as originating from an amorphous NiO-like species on $TiO_2$, in agreement with the UV-Vis data of FIG. 4A. FIG. 12 are XPS Ti 2p spectra for the photocatalyst precursor, photocatalyst and reference materials. Spectra 1202 is a XPS Ti 2p spectra for the support material. Spectra 1214 and 1216 a XPS Ti 2 p spectra for the photocatalyst precursor Samples 8 and 9, respectively. These spectra all show characteristic peaks for $Ti^{4+}$ in $TiO_2$ with the expected decrease in intensity with increase in Ni content. Ni (II) is paramagnetic, which gives rise to additional "shake-up" satellite features ~ 6 eV above the main Ni $2p_{1/2}$ and $2p_{3/2}$ lines.

**[0080] Photocatalyst**. Spectra 1104 of FIG. 11 is a Ni 2p XPS spectra of photocatalyst Sample 19. Spectra 1204-1212 of FIG. 12 are XPS TI 2p spectra for photocatalyst Samples 15-19, respectively. Referring to spectra 1104 of FIG. 11, it can be determined that following $H_2$ reduction at 500 $^oC$, metallic Ni was the dominant Ni species on the surface of the photocatalysts as the Ni $2p_{3/2}$ and Ni $2p_{1/2}$ of 853.2 eV and 870.5 eV, respectively, were almost identical to those measured for an $Ar^+$ sputtered Ni foil shown in spectra 1106. The weak peaks ~5.7 eV above the Ni 2p peaks were assigned to surface plasmon loss features. A modified Auger parameter ($\alpha'$) to discriminate Ni from NiO. The modified Auger

parameters determined for the Ni foil (Sample 22) and the photocatalyst Sample 19 (calculated using the Ni $2p_{3/2}$ and $L_3M_{45}M_{45}$ Auger energies), were 1698.8 eV and 1698.9 eV, respectively, and in good agreement with known values of 1698.8 eV for metallic Ni (c.f. NiO, $\alpha' = 1697.7$ eV). Spectra 1204-1210 are XPS Ti 2p spectra of photocatalysts Samples 15-19, respectively. These spectra all show characteristic peaks for $Ti^{4+}$ in $TiO_2$ with the expected decrease in intensity with increase in Ni content.

## F. Ni L-edge NEXAFS

**[0081]** Ni L-edge Near Edge X-ray Absorption Fine Structure (NEXAFS) was used to analyse the photocatalyst precursors and the photocatalysts of the present invention. The NEXAFS data was obtained by using the procedures discussed above in Section E (X-ray Photoelectron Spectroscopy (XPS).

**[0082]** **Photocatalyst Precursor**. FIG. 13 are Ni L-edge spectra of the photocatalyst precursor, photocatalyst, and reference material. Spectra 1302 is a Ni L-edge spectrum for photocatalyst precursor Sample 9. Spectra 1308 is a Ni L-edge spectrum for nickel oxide. Comparing spectra 1302 to spectra 1309, photocatalyst precursor Sample 9 was identical in most respects to that collected for the NiO reference sample. Thus, NiO was the nickel-containing precursor species on the $TiO_2$ support.

**[0083]** **Photocatalyst.** Spectra 1304 in FIG. 13 is the N L-edge NEXAFS spectrum of photocatalyst Sample 19, and was qualitatively similar to spectra 1306 collected for the $Ar^+$ sputtered Ni foil, which is dominated by peaks at 854.6 eV and 871.9 eV assigned to $L_3$ (Ni $2p_{3/2} \rightarrow$ Ni 3d transitions) and $L_2$ (Ni $2p_{1/2} \rightarrow$ Ni 3d transitions) features, respectively. Additional weak features on the high energy side of the $L_3$ and $L_2$ features suggest the presence of a small Ni(II) component, presumably NiO formed be brief exposure of the sample to air following the $H_2$ reduction step. NEXAFS for the other $Ni/TiO_2$ samples (not shown), showed a progressive increases in the integrated area of the Ni L-edge features with nominal metal loading.

## G. $N_2$ Physisorption Isotherms

**[0084]** Nitrogen physisorption (physical adsoption) isotherms were determined at liquid nitrogen temperature (-195 °C) using a Micromeritics Tristar 3000 instrument. Specific surface areas were calculated from the $N_2$ adsorption data according to the Brunauer-Emmett-Teller (BET) method using $P/P_o$ values in the range 0.05-0.2. Cumulative pore volumes and pore diameters were calculated from the adsorption isotherms by the Barrett-Joyner-Halenda

(BJH) method. Samples were degassed at 100 °C under vacuum for 1 h prior to the $N_2$ physisorption measurements. Table 1 summarizes $N_2$ physisorption data for the Ni/$TiO_2$ photocatalysts. All samples had similar $N_2$ physisorption isotherms that could be classified as Type II accordingly to the IUPAC convention for adsorption isotherms. The BET surface area, BJH cumulative pore volumes and pore diameters of the photocatalysts of the invention were all similar and appear to be independent the Ni loading.

## H. Photoluminescence

**[0085]** Photoluminescence measurements were performed in air at room temperature using a Perkin-Elmer LS-55 Luminescence Spectrometer. A 290 nm cut-off filter was used. Spectra were excited at 310 nm and photoluminescence spectra were recorded over a range of 330-600 nm using a standard photomultiplier.

**[0086]** **Photocatalyst Precursor.** FIG. 14 are photoluminescence spectra of the support material (P25 $TiO_2$, data line 1402), and the photocatalyst precursor material Samples 3, 5, and 7-9, (data lines 1404, 1406, 1408, 1410, and 1412, respectively) that were collected in air. P25 $TiO_2$ gave a very intense and broad photoluminescence signal centred around 390 nm, which contained contributions from direct and indirect transitions in anatase and rutile (mainly the former since by weight anatase is the dominant $TiO_2$ polymorph in P25 $TiO_2$). Additional sharper features at lower energies were assigned recombination events involving surface traps. The high intensity of the photoluminescence signal observed for P25 $TiO_2$ indicates rapid electron-hole pair recombination occurs following UV excitation. Following deposition of NiO on P25 $TiO_2$, the photoluminescence signal observed was weaker, confirming that NiO effectively suppresses electron-hole pair recombination in $TiO_2$, even at low NiO loadings (see FIG. 14 inset). Presumably NiO is scavenging electrons promoted into the conduction band of $TiO_2$, resulting in the reduction of NiO to Ni.

**[0087]** **Photocatalyst.** FIG. 15 are photoluminescence spectra of the support material (data line 1502) and the photocatalyst Samples 13, 15, and 17-19 (data lines 1504, 1506, 1508, 1510, and 1512, respectively. As shown in the FIG. 15 insert, the photoluminescence signal for the Ni/$TiO_2$ photocatalysts was even weaker than those for the photocatalyst precursor, which supported the belief that metallic Ni is a more effective acceptor of electrons from $TiO_2$ than NiO.

**Table 2**

| Sample No. | Samples | Ni content by XRF (wt.%) | XRF Ni:Ti (wt. ) | Bandgap (eV) | BET surface area ($m^2 g^{-1}$) | Atom% by XPS | | | | | |
|---|---|---|---|---|---|---|---|---|---|---|---|
| | | | | | | Ti | O | C | Ni | O:Ti | Ni:Ti |
| 0 | P25 $TiO_2$ Support | 0.0 | 0 | 3.15 | 49.1 | 26.1 | 53.5 | 20.4 | - | 2.00 | 0.00 |
| 12 | 0.13 wt.% Ni/$TiO_2$ | 0.2 | 0.00334 | 2.96 | 46.0 | - | - | - | - | - | - |
| 13 | 0.25 wt.% Ni/$TiO_2$ | 0.2 | 0.00334 | 2.94 | 44.3 | - | - | - | - | - | - |
| 14 | 0.38 wt.% Ni/$TiO_2$ | 0.4 | 0.00670 | 2.90 | 43.3 | - | - | - | - | - | - |
| 15 | 0.5 wt.% Ni/$TiO_2$ | 0.5 | 0.00838 | 2.84 | 44.9 | 25.1 | 53.6 | 20.8 | 0.6 | 2.14 | 0.03 |
| 16 | 0.75 wt.% Ni/$TiO_2$ | 0.7 | 0.01176 | 2.83 | 46.0 | 26.1 | 51.4 | 21.6 | 0.9 | 1.97 | 0.03 |
| 17 | 1 wt.% Ni/$TiO_2$ | 1.1 | 0.02026 | 2.81 | 45.7 | 27.4 | 52.0 | 19.6 | 1.0 | 1.90 | 0.04 |
| 18 | 2 wt.% Ni/$TiO_2$ | 1.9 | 0.03231 | 2.78 | 46.0 | 26.3 | 51.9 | 20.3 | 1.5 | 1.97 | 0.06 |
| 19 | 4 wt.% Ni/$TiO_2$ | 3.8 | 0.06591 | 2.76 | 43.8 | 26.6 | 51.9 | 19.7 | 1.8 | 1.95 | 0.07 |
| 5 | 0.63 wt.% NiO/$TiO_2$ | 0.5 | 0.00838 | 2.66 | 48.9 | - | - | - | - | - | - |
| 9 | 5 wt.% NiO/$TiO_2$ | - | | 2.65 | 52.8 | 25.1 | 50.6 | 18.5 | 5.9 | 2.02 | 0.24 |
| 22 | Ni foil ($Ar^+$ sputtered) | - | | - | - | - | 3.3 | 1.1 | 95.6 | - | - |
| 10 | NiO | - | | - | 0.4 | - | 49.9 | 11.6 | 38.6 | - | - |
| 21 | $NiTiO_3$ | - | | - | - | 13.9 | 57.6 | 13.6 | 15.0 | 4.14 | 1.08 |
| | 2 wt.% Au/$TiO_2$ | 2.2 | | 2.95 | 47.6 | 20.9 | 50.4 | 28.3 | - | 2.41 | - |

## Example 3
## (Use of Photocatalysts in Water-Splitting Reactions)

**[0088] Experimental Set-Up:** Catalytic reactions were conducted in a borosilicate (Pyrex®, Corning) glass reactor having a capacity of 100 mL. For each experiment, a photocatalyst (6.5 mg) was added to the glass reactor and evacuated under a nitrogen flow for 30 minutes to remove oxygen. An ethanol/water mixture (20 mL water, 80 vol.% ethanol) was added to the oxygen free reactor. The resulting photocatalyst dispersion was stirred continuously for 1 hour in the dark (no UV excitation). The reaction mixture was irradiated with sunlight, with a light flux at the front side of the reactor of between 0.3 and 1 $mW/cm^2$. The mixture containing photocatalyst, water and sacrificial agent was stirred constantly under dark conditions to disperse the catalyst and sacrificial agent in the water. The reactor was then exposed to a UV light, supplied from a Spectraline model SB-100P/F lamp (100 W, 365 nm) at a distance of 10 cm from the reactor. The photon flux at the sample was approximately 6.5 mW $cm^{-2}$ (the UV flux from the Sun is approximately 5 mW $cm^{-2}$). Hydrogen evolution was monitored by taking gas head space samples (1 mL) at 20 min intervals and injecting these into a Shimadzu GC 2014 equipped with a TCD detector and Carboxen-1010 plot capillary column (L×I.D. 30 m×0.53 mm, average thickness 30 μm). $H_2$ evolved was quantified against an external calibration curve of peak area versus moles of $H_2$.

**[0089] Water-Splitting Reactions.** Table 3 lists the rate of hydrogen ($H_2$) production for the photocatalysts of the present invention (Samples 12-19), a photocatalyst precursor (Sample 5), support material (Sample 1), and a photocatalyst containing gold. FIG. 16 are plots of $H_2$ production versus time for the support material (Sample 1, P25 $TiO_2$, data line 1602), the photocatalyst of the present invention (Samples 12-17, data lines 1604, 1606, 1608, 1610, 1612, and 1614, respectively) and the gold containing photocatalyst (data line 1616). P25 $TiO_2$ showed low activity for $H_2$ production ($H_2$ production rate 1.2 mmol $h^{-1}$ $g^{-1}$), due to rapid electron-hole pair recombination following UV excitation in the absence of added co-catalyst. Notably, the catalysts of the present invention are more active than the Au catalysts at both ends for the x axis, in particular at very small % of ethanol in water.

**[0090]** Sample 15 (0.5 wt.% $Ni/TiO_2$) photocatalyst exhibited the highest activity ($H_2$ production rates = 32.4 $mmolg^{-1}h^{-1}$ and 20.7 $mmolg^{-1}h^{-1}$, respectively, at an 80:20 vol.% EtOH:$H_2O$ ratio) of the nickel photocatalyst. The photocatalysts of the present invention showed stable $H_2$ production activities, as evidenced by the linearity of the plots in FIG. 16.

Extended experiments over a 24 h period for selected catalysts showed the same linearity (not shown).

**[0091]** FIG. 17 are plots of hydrogen production versus time for the catalyst precursor Sample 5 (data line 1702) and a photocatalyst Sample 15 (data line 1704) in an 80:20 vol.% ethanol to water solution under UV irradiation. The catalyst precursor Sample 5 is the precursor to sample 15 prior to being reduced. The catalyst precursor Sample 5 had a 90 min induction period before any meaningful rate of $H_2$ production is achieved. Without wishing to be bound by theory, it is believed that the induction period corresponds to the photocatalytic reduction of NiO to $Ni^0$, with the $Ni^0$ providing the active sites for $H_2$ evolution. Since the slope of the line following the induction period for Sample 5 was lower than that observed for Sample 15 which was pre-reduced in $H_2$ at 500 $^oC$, it can be concluded that only a fraction of the surface NiO has been reduced to $Ni^0$ (theoretically if all the NiO had been reduced, the $Ni^0$ loading would be 0.5 wt.%).

**[0092]** **Hydrogen Production As A Function Of Weight Percent Nickel.** FIG. 18 are plots of hydrogen production versus nickel concentration in the photocatalyst in weight percent at ethanol to water volume percent ratios of 80:20(data line 1802) and 90:10 (data line 1804). From FIG. 18, it was determined that a nickel loading of 0.5 wt.% was produced the highest amount of hydrogen at the EtOH:$H_2O$ volume percent ratios of 10:90 and 80:20. The same general trend was seen when the $H_2$ production rates were normalised against photocatalyst surface area (Table 2, mmol $g_{Ni}^{-1}$ $h^{-1}$). It was observed that at Ni loadings above 0.5 wt.%, the rates of $H_2$ production decreased sharply. Without wishing to be bound by theory, it is believed that the decrease in the activity of the Ni/$TiO_2$ photocatalysts above the Ni loading of 0.5 wt.% was due to excessive blockage of $TiO_2$ sites (where ethanol and water photo-oxidation occur) by the highly dispersed metallic Ni nanoparticles. The fact that the Ni/$TiO_2$ photocatalysts show very good activities for $H_2$ production at low metal loadings makes the photocatalyst of the present invention suitable for large scale solar $H_2$ generation.

**[0093]** **Hydrogen Production As A Function Of Ethanol Concentration.** FIG. 19 are plots of $H_2$ production rates versus inverse normalized photoluminescence intensities from photocatalyst Sample 15 (0.5 wt.% Ni/$TiO_2$) at volume ratios of ethanol to water of 80:20 (data line 1902) and 10:90 (data line 1904). At both ethanol to water ratios, a reasonably linear relationship is found, providing strong evidence that metallic Ni promotes $H_2$ generation through supressing electron-hole pair recombination in $TiO_2$. FIG. 20 are plots of hydrogen production rate under UV conditions in mmol $g^{-1}$ $h^{-1}$ versus concentration of

ethanol in volume percent for two photocatalysts Samples 14 and 15. From FIG. 20, it was determined that the activity of the Sample 15 photocatalyst (0.5 wt.% $Ni/TiO_2$, data line 2002) increased with ethanol concentration up to 95 vol.% ethanol, before dropping sharply at 100 vol.% ethanol. The activity of the Sample 15 photocatalysts was better than the performance of the Sample 14 photocatalyst (0.38 wt.% $Ni/TiO_2$, data line 2004), and comparable to the 2 wt.% $Au/TiO_2$ reference photocatalyst, at low ethanol-concentrations (data line 2006). It should be noted that 2 wt.% is the optimum Au loading in the $Au/TiO_2$ system. At low ethanol concentrations (< 15 vol.%) and high ethanol concentrations (> 90 vol%), the activity of the Sample 15 photocatalyst (data line 2002) was superior to that of the $Au/TiO_2$ photocatalyst (data line 2006). This was a uprising and unexpected result. It is believed that the activities (~ 10 mmol $g^{-1}$ $h^{-1}$) for the Sample 15 photocatalyst (0.5 wt.% $Ni/TiO_2$) at low ethanol concentrations (e.g. <5 vol. % EtOH) are amongst the highest for a $TiO_2$-based photocatalyst system that doesn't contain Pd, Pt or Au.

**Table 3**

| Sample No. | Metal or Metal oxide, wt.% | $H_2$ production rate 10 vol.% EtOH: 90 vol.% $H_2O$ | | | $H_2$ production rate 80 vol.% EtOH: 20 vol.% $H_2O$ | | |
|---|---|---|---|---|---|---|---|
| | | mmol $g^{-1}$ $h^{-1}$ | mmol $m^{-2}$ $h^{-1}$ | mmol $g_{Ni}^{-1}$ $h^{-1}$ | mmol $g^{-1}$ $h^{-1}$ | mmol $m^{-2}$ $h^{-1}$ | mmol $g_{Ni}^{-1}$ $h^{-1}$ |
| 1 | 0% | 0.5 | 0.006 | - | 1.2 | 0.024 | - |
| 12 | 0.13 | 2.5 | 0.054 | 1.92 | 11.7 | 0.254 | 9.00 |
| 13 | 0.25 | 5.1 | 0.115 | 2.04 | 16.6 | 0.375 | 6.64 |
| 14 | 0.38 | 5.8 | 0.134 | 1.53 | 17.6 | 0.406 | 4.63 |
| 15 | 0.5 | 11.6 | 0.258 | 2.32 | 20.7 | 0.461 | 4.14 |
| 16 | 0.75 | 5.5 | 0.120 | 0.73 | 16.6 | 0.361 | 2.21 |
| 17 | 1 | 4.3 | 0.094 | 0.43 | 15.4 | 0.337 | 1.54 |
| 18 | 2 | 3.5 | 0.076 | 0.18 | 12.9 | 0.280 | 0.65 |
| 19 | 4 | 2.9 | 0.066 | 0.07 | 5.4 | 0.123 | 0.14 |
| 5 | 0.63 | - | - | - | 4.8 | 0.098 | 0.76 |
| Gold | 2 | 9.3 | 0.195 | - | 32.4 | 0.681 | - |

## CLAIMS

1. A photocatalyst comprising Ni(0) dispersed on a titanium dioxide support, said photocatalyst having a Ni(0) content of greater than 0 to 4 wt. %, as determined by X-ray fluorescence (XRF), wherein the Ni(0) is dispersed on the titanium dioxide support in the form of particles having an average particle size of less than or equal to 1 nm.

2. The photocatalyst of claim 1, wherein the photocatalyst has a Brunauer-Emmett-Teller (BET) surface area of 43 to 46 $m^2g^{-1}$, a Ni(0) to Ti atom % of greater than 0 to 0.07, as determined by X-ray photoelectron spectroscopy (XPS), or both.

3. The photocatalyst of claim 1, wherein the Ni(0) content is 0.1 to 4 wt. %, preferably 0.2 to 2 wt. %, or more preferably 0.4 to 0.8 wt.%, or most preferably 0.4 to 0.6 wt. %.

4. The photocatalyst of claim 3, wherein the Ni(0):Ti atom % is 0.03 to 0.04.

5. The photocatalyst of claim 1, wherein the Ni(0) is obtained, *in situ*, from $H_2$ reduction of NiO.

6. The photocatalyst of claim 1, wherein the titanium dioxide comprises anatase, rutile, brookite, or any combination thereof, preferably single phase anatase.

7. The photocatalyst of claim 1, wherein the photocatalyst does not include any one of gold, ruthenium, rhenium, rhodium, palladium, silver, copper, osmium, iridium, and platinum.

8. The photocatalyst of claim 1, wherein the photocatalyst is comprised in a composition that includes water.

9. A system for producing hydrogen gas and oxygen gas from water, the system comprising:

   (a) a transparent container comprising a composition that includes the photocatalyst of any one of claims 1 to 15, water, and a sacrificial agent; and

   (b) a light source for irradiating the composition.

10. The system of claim 16, wherein the light source is sunlight, an ultra-violet lamp, or an ultra-violet/visible lamp.

11. A method for producing hydrogen gas and oxygen gas from water, the method comprising obtaining a system of any one of claims 9 to 10 and subjecting the composition to the light source for a sufficient period of time to produce hydrogen gas and oxygen gas from the water.

12. A method of making any one of the photocatalysts of claims 1 to 7, the method comprising:

a. obtaining a titanium dioxide support material having a Ni(II) complex dispersed on the support material; and

b. heating the titanium dioxide support material and reducing the Ni(II) to Ni(0) with a gas comprising $H_2$ to form the photocatalyst.

13. The method of claim 12, wherein the Ni(II) in step b is NiO.

14. The method of claim 12, wherein the gas further comprises $N_2$.

15. The method of claim 12, wherein the titanium dioxide support material is heated at a temperature of 350 $^{o}$C to 700 $^{o}$C for at least one hour or the titanium dioxide support material is heated at a temperature of 450 $^{o}$C to 550 $^{o}$C for 1 to 3 hours or for 2 hours.

16. The method of claim 12, wherein obtaining the titanium dioxide support material comprises forming the Ni(II) complex on the support material.

17. The method of claim 16, wherein forming the Ni(II) complex on the support material comprises:

(i) combining a nickel (II) salt and glycerol with water to form an aqueous solution of a Ni(II)-glycerol complex;

(ii) adding titanium dioxide support material to the solution;

(iii) precipitating the Ni(II)-glycerol complex on the titanium dioxide support material with a basic media to form a mixture;

(iv) agitating the mixture;

(v) removing all or substantially all the liquids from the mixture and collecting the solids;

(vi) washing the solids with water; and

(vii) drying and calcining the solids.

18. The method of claim 17, wherein the step of precipitating the Ni(II)-glycerol complex on the $TiO_2$ support material by the addition of basic media comprises dropwise addition of an aqueous solution of NaOH with stirring until the mixture attains a pH of about 12.

19. The method of claim 18, wherein the solids comprise $Ni(OH)_2/TiO_2$.

20. The method of claim 17, wherein said calcining comprises heating at a temperature of 300 $^{o}$C for two hours in air to form NiO.

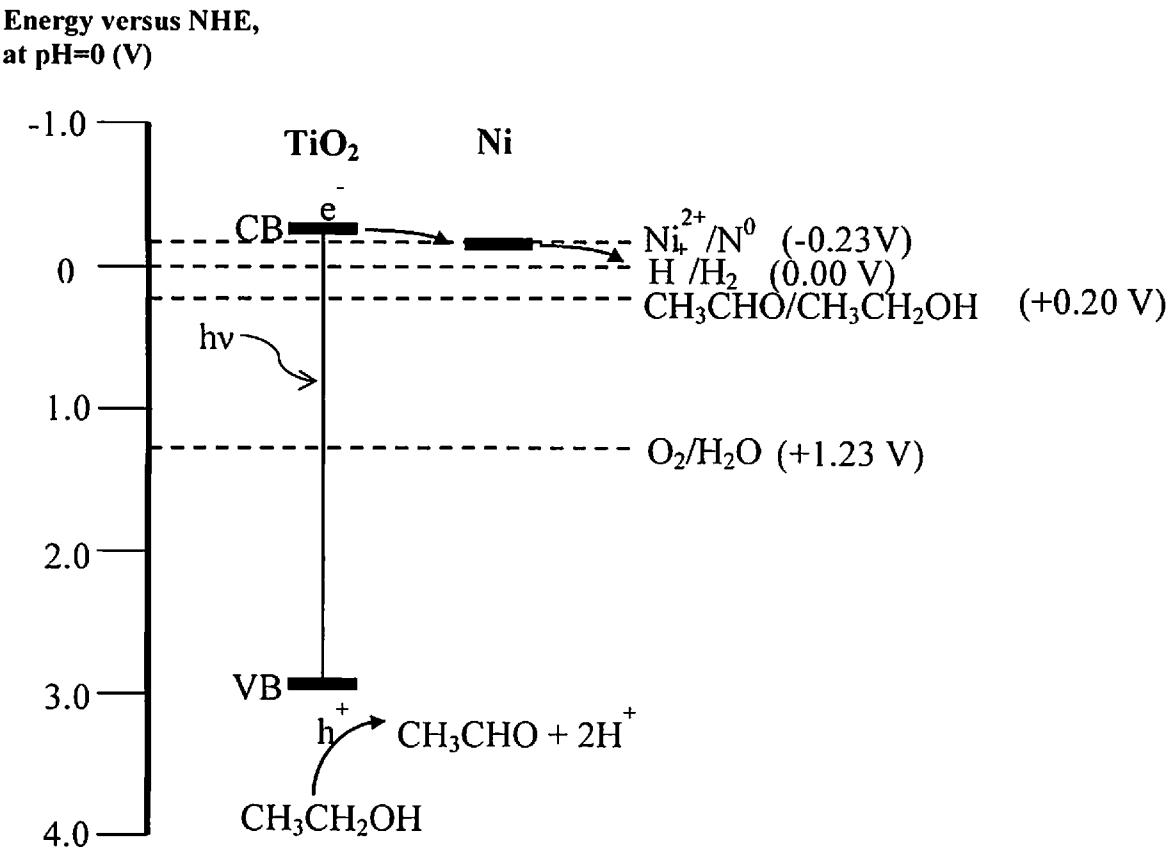
Energy versus NHE,
at pH=0 (V)
-1.0
0
1.0
2.0
3.0
4.0
TiO2
Ni
e-
CB
VB
hν
h+
Ni2+/N0 (-0.23V)
H+/H2 (0.00 V)
CH3CHO/CH3CH2OH (+0.20 V)
O2/H2O (+1.23 V)
CH3CHO + 2H+
CH3CH2OH

FIG. 1

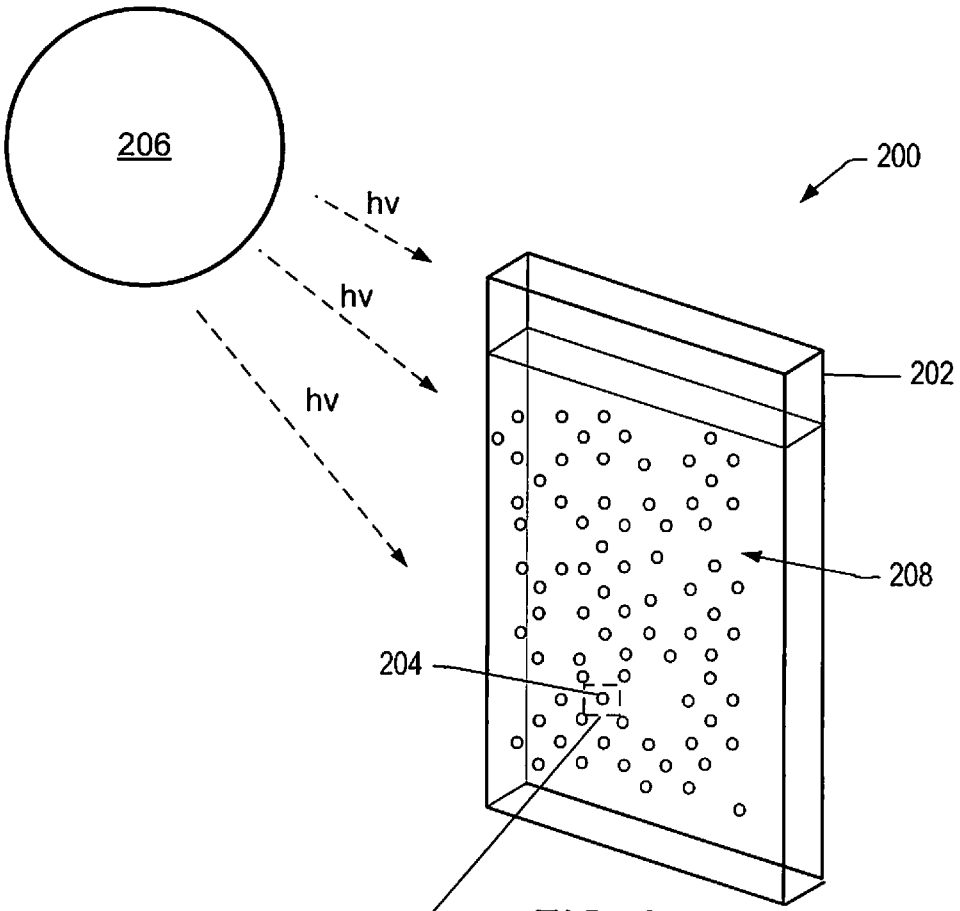


FIG. 2

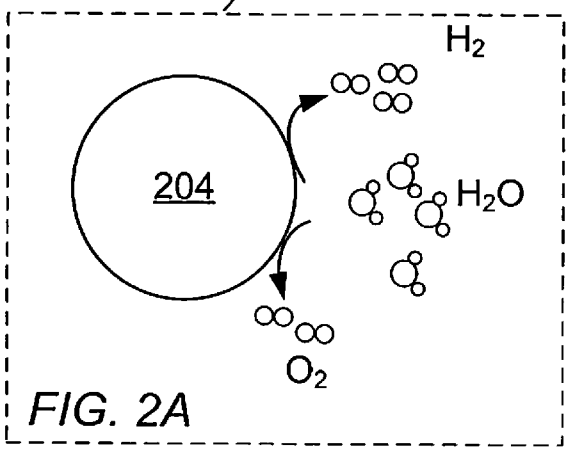


FIG. 2A

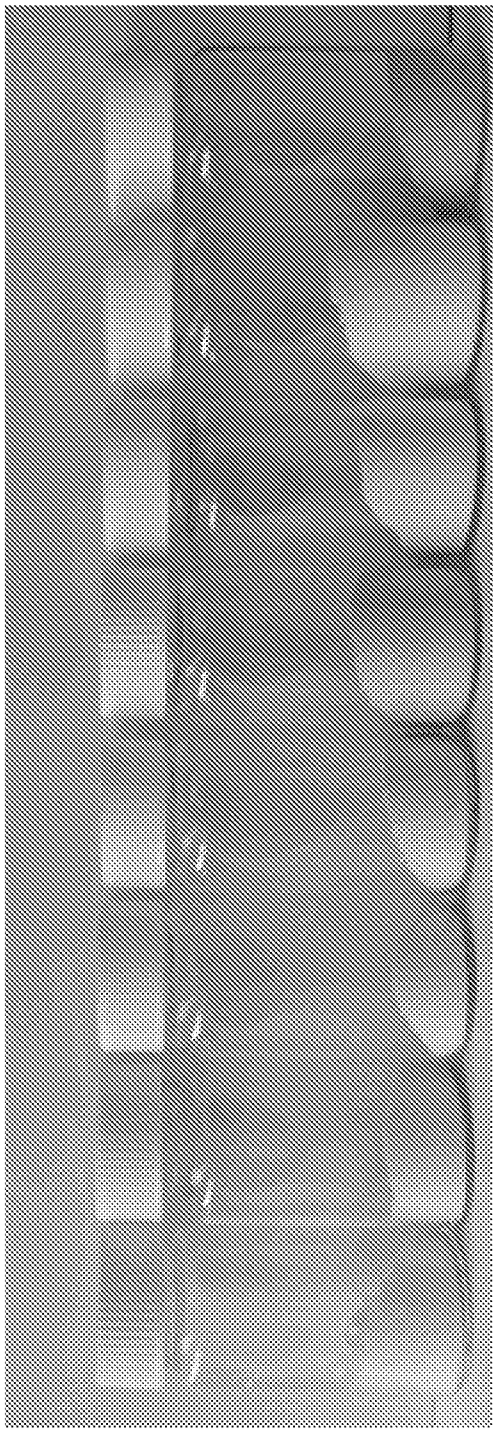

FIG. 3A

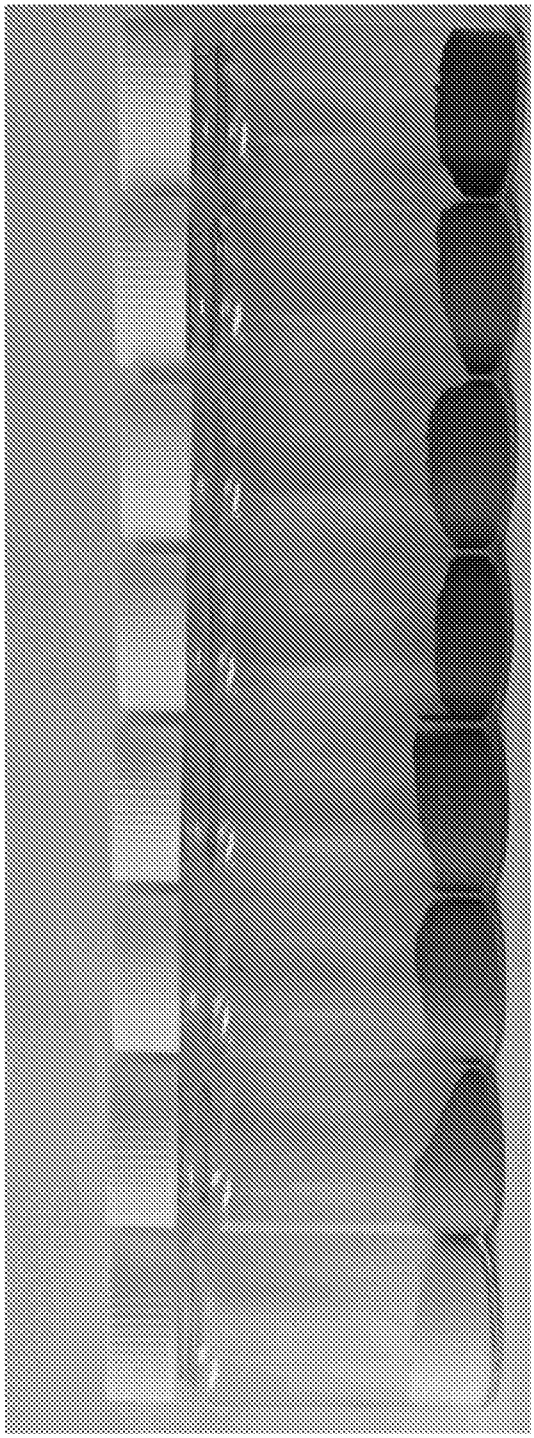

FIG. 3B

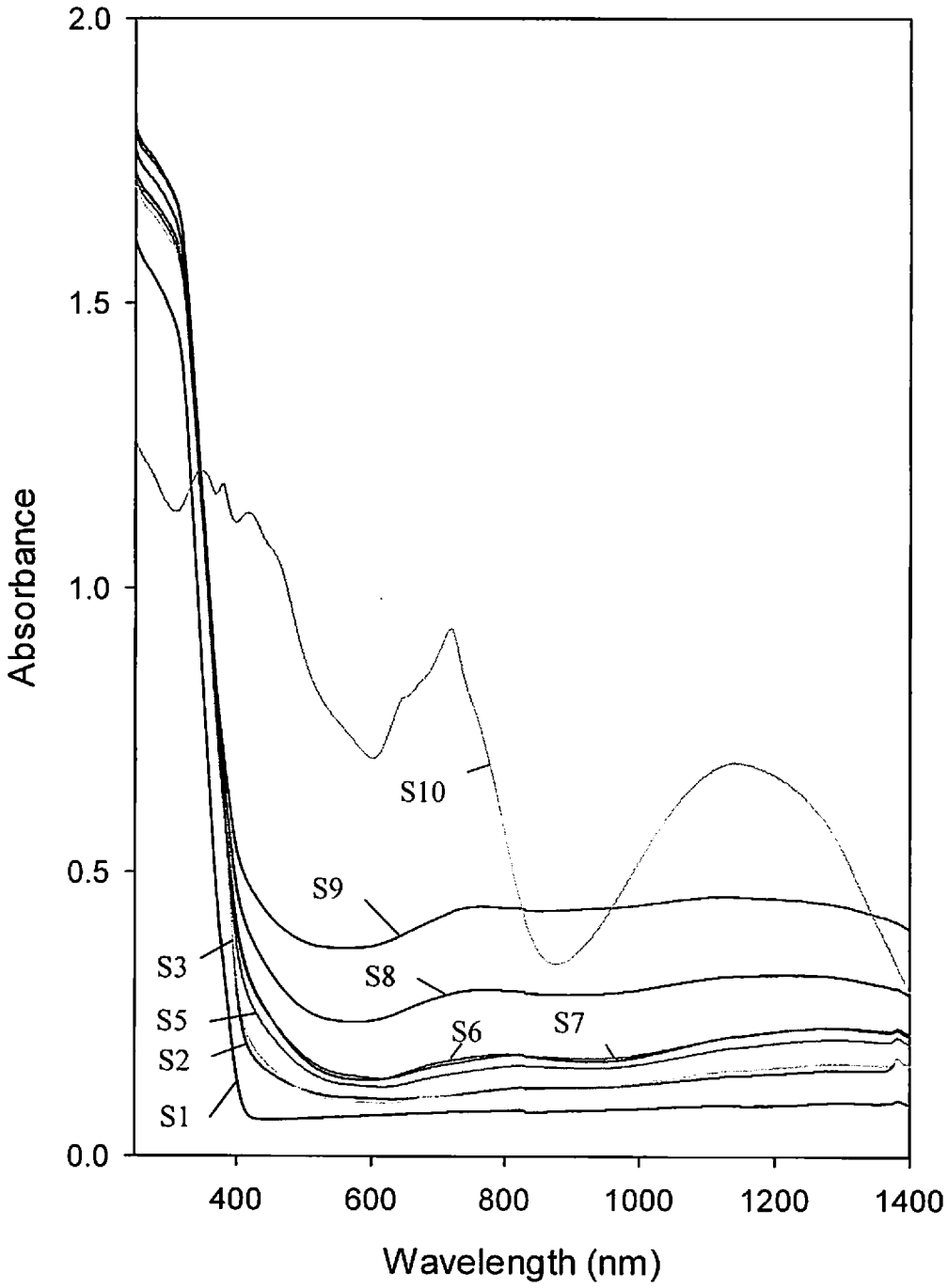
2.0
1.5
1.0
0.5
0.0
Absorbance
400
600
800
1000
1200
1400
Wavelength (nm)
S10
S9
S8
S7
S6
S5
S3
S2
S1

*FIG. 4A*

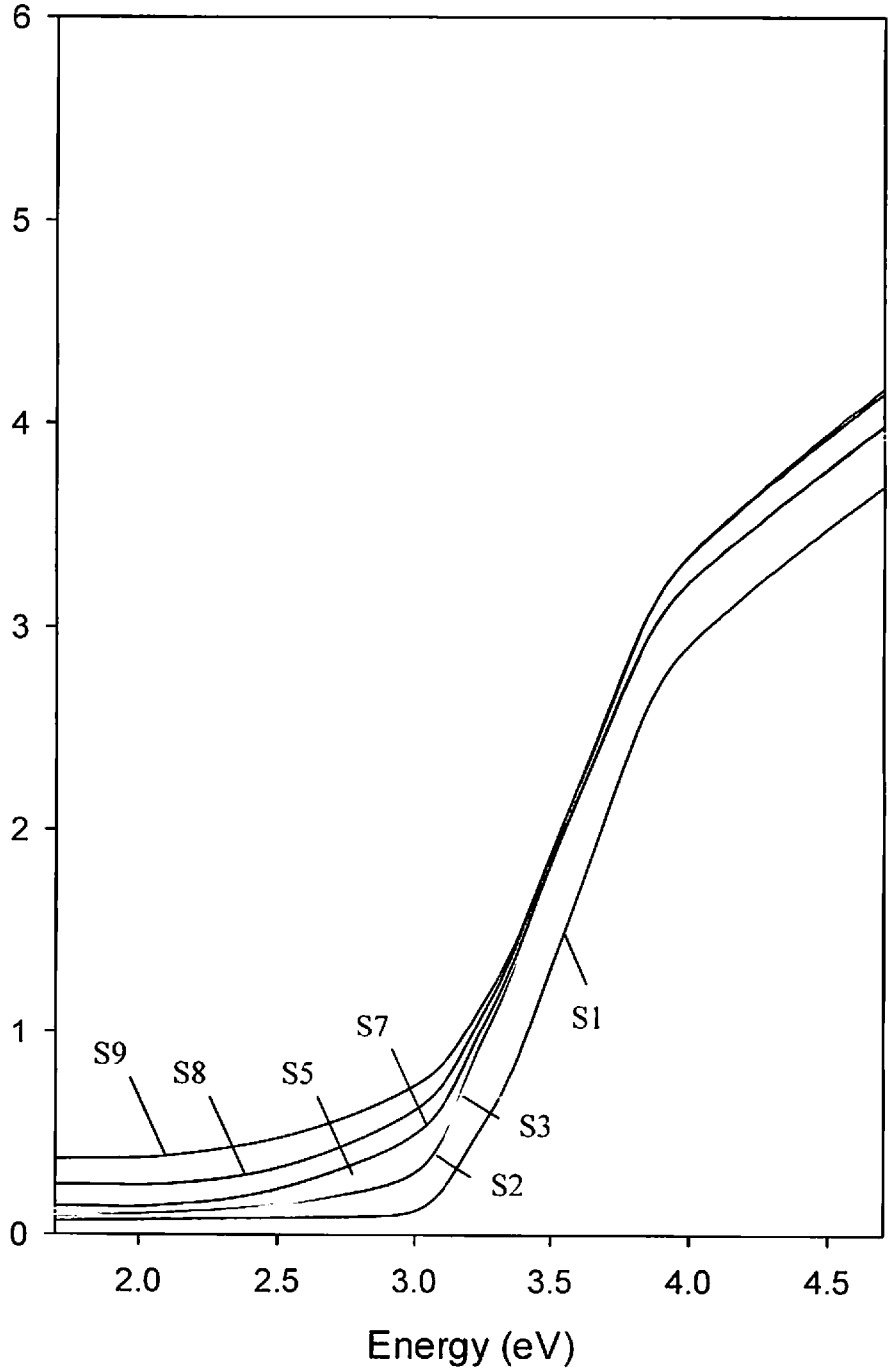


*FIG. 4B*

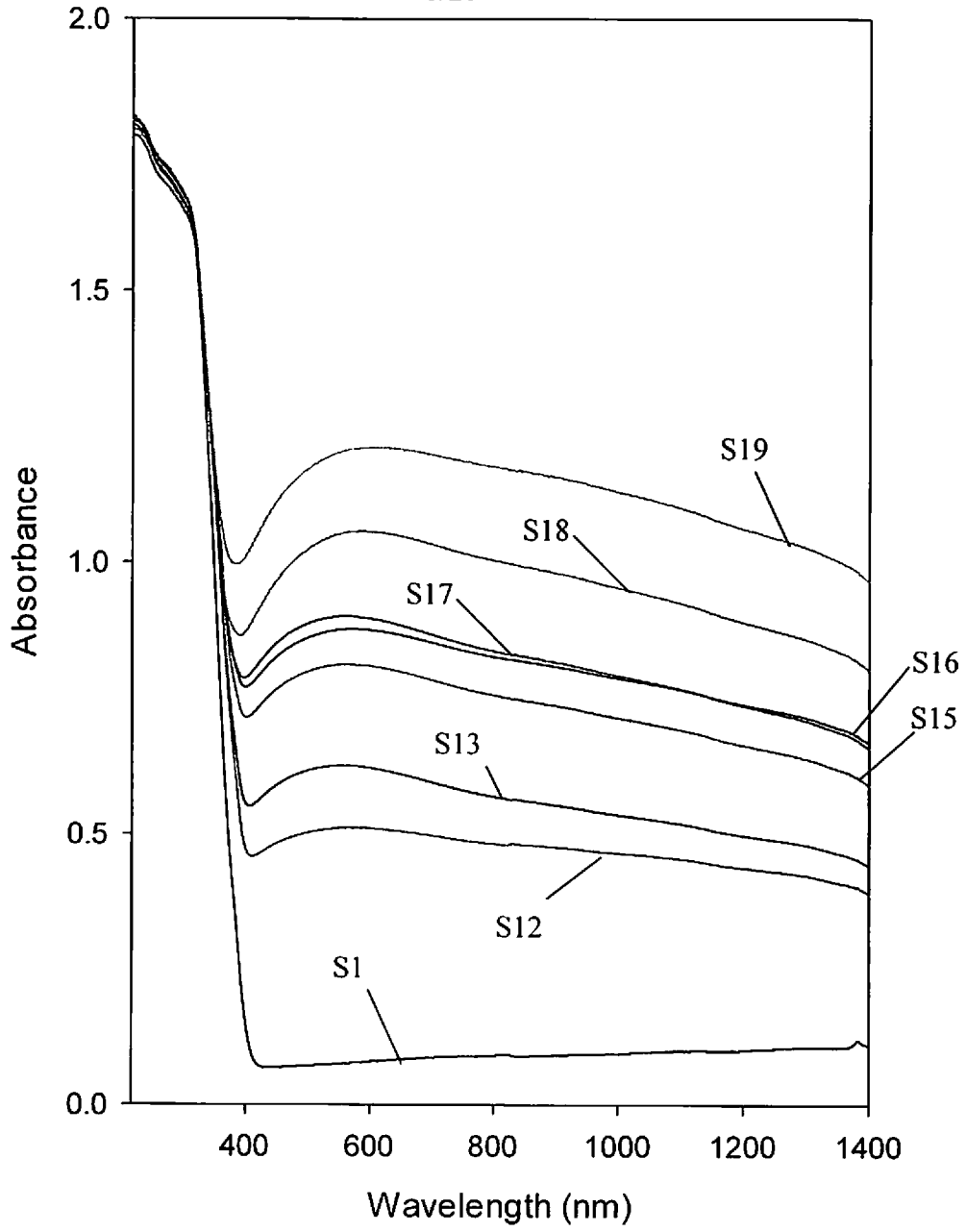
2.0
1.5
1.0
0.5
0.0
Absorbance
400
600
800
1000
1200
1400
Wavelength (nm)
S19
S18
S17
S16
S15
S13
S12
S1

*FIG. 5A*

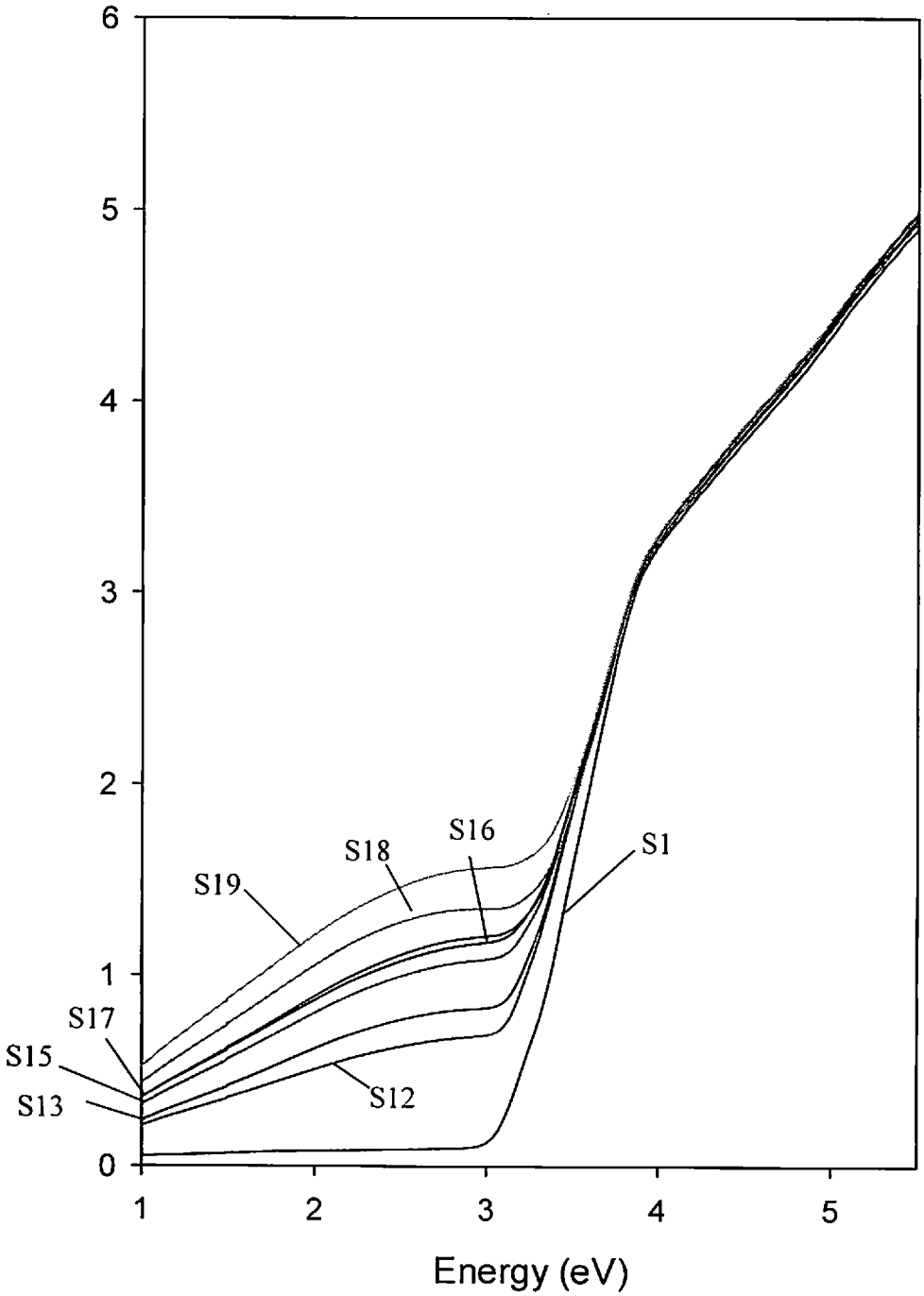


*FIG. 5B*

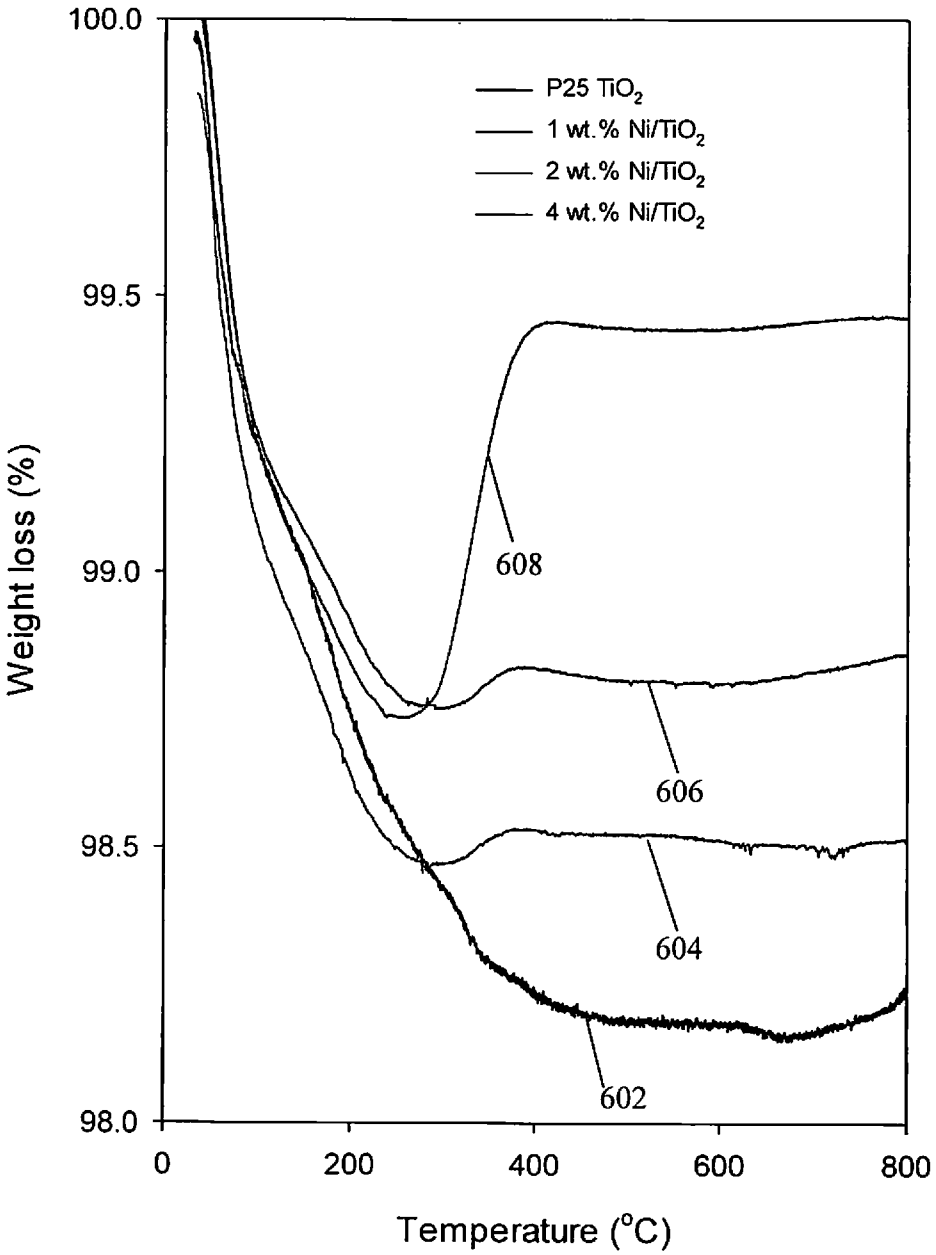
100.0
99.5
99.0
98.5
98.0
Weight loss (%)
0
200
400
600
800
Temperature (°C)
P25 TiO2
1 wt.% Ni/TiO2
2 wt.% Ni/TiO2
4 wt.% Ni/TiO2
608
606
604
602

*FIG. 6*

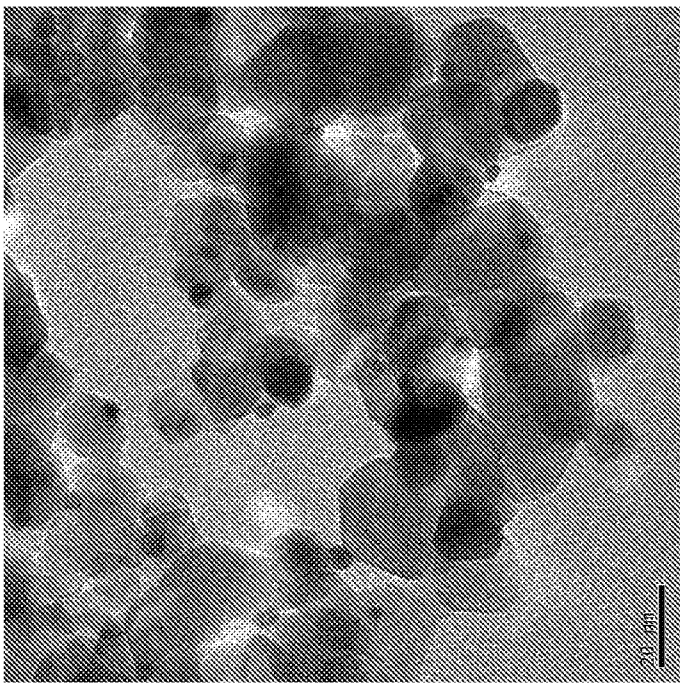


FIG. 8

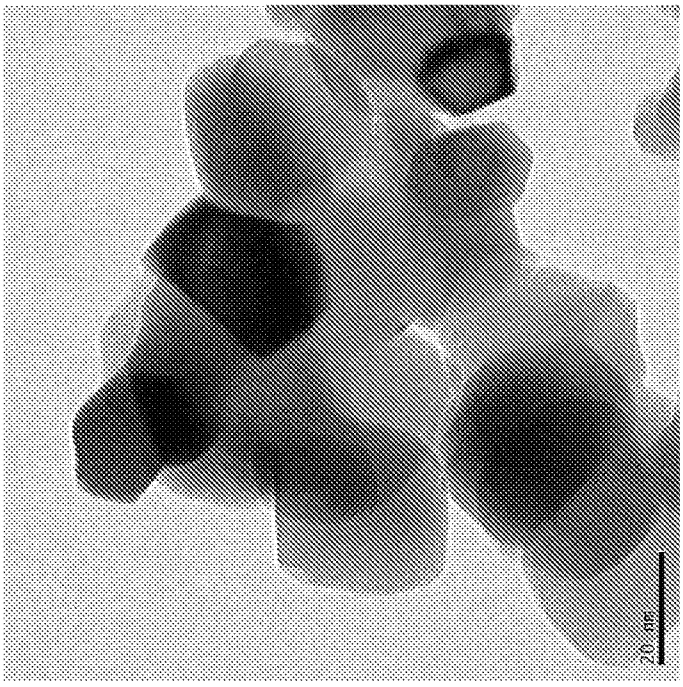


FIG. 7

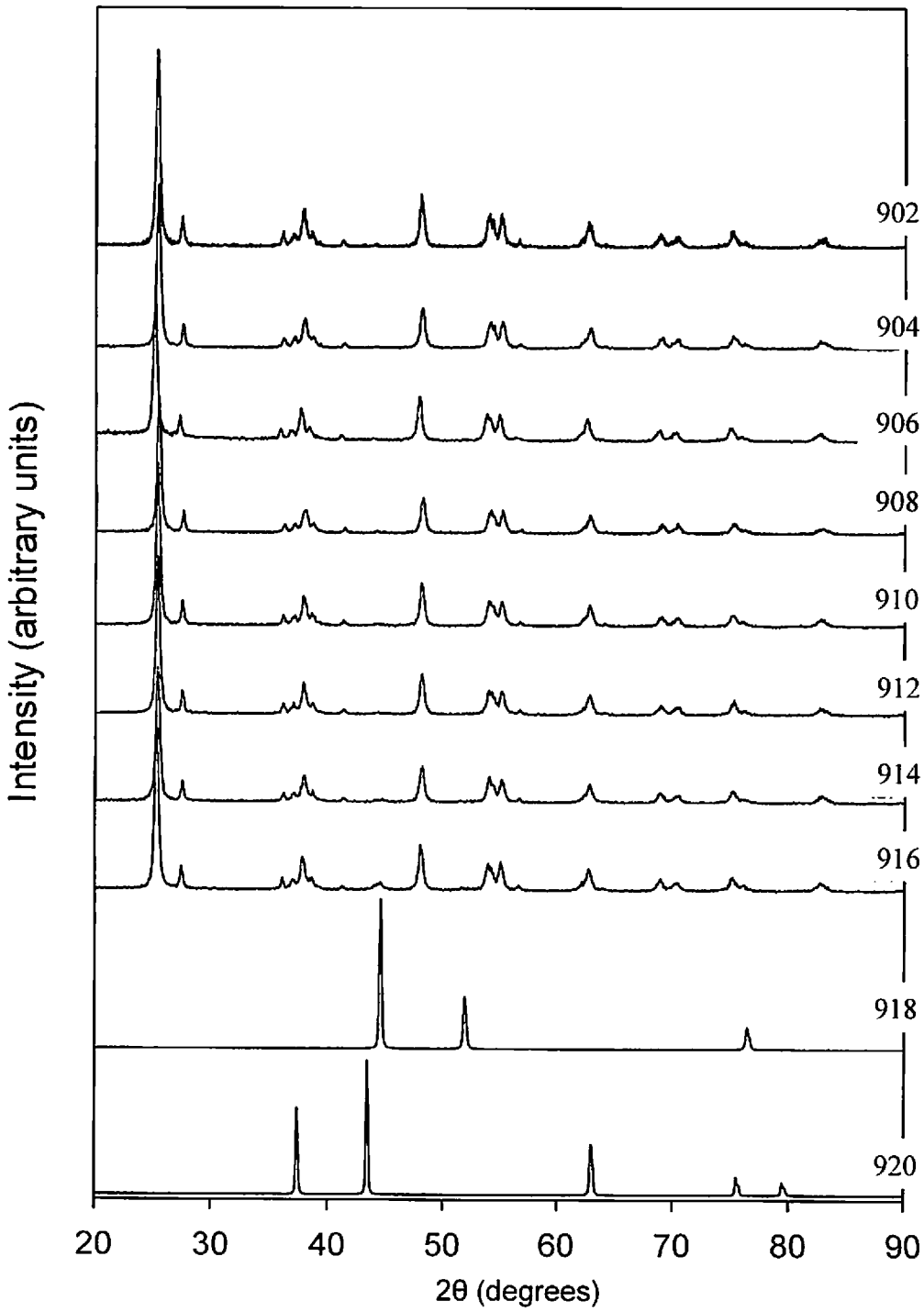
Intensity (arbitrary units)
902
904
906
908
910
912
914
916
918
920
20
30
40
50
60
70
80
90
2θ (degrees)

*FIG. 9*

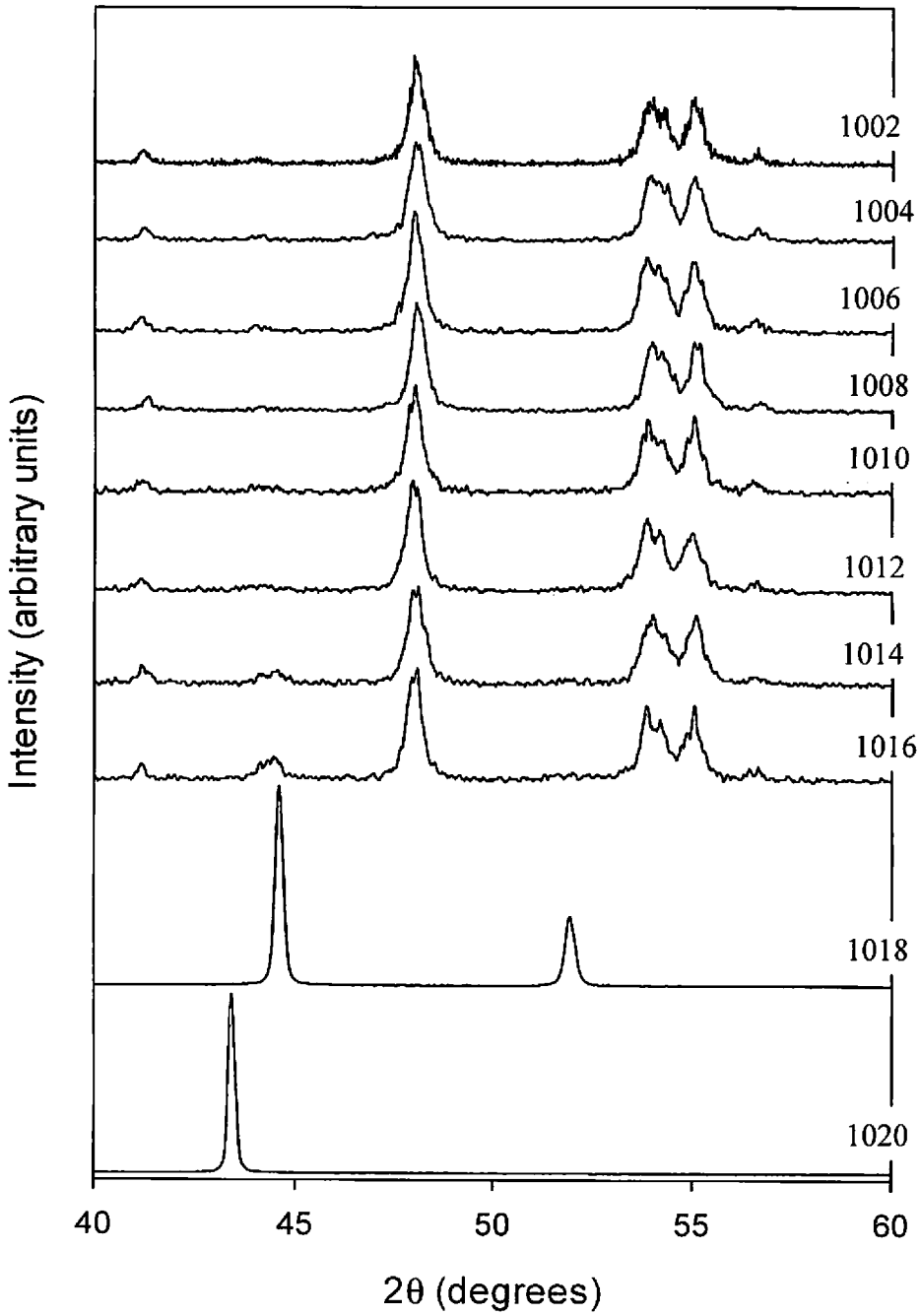
1002
1004
1006
1008
1010
1012
1014
1016
1018
1020
Intensity (arbitrary units)
40
45
50
55
60
2θ (degrees)

*FIG. 10*

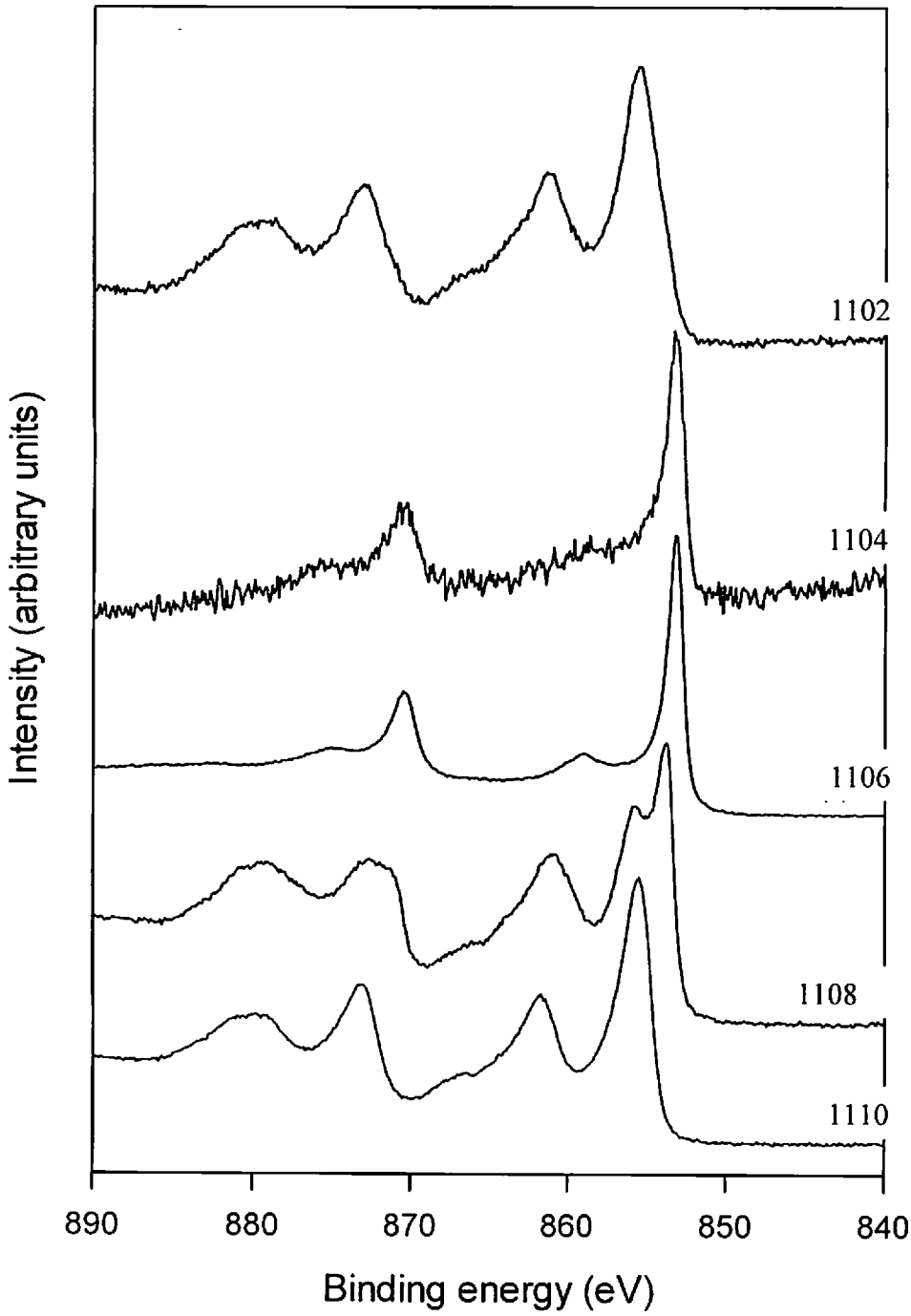
Intensity (arbitrary units)
1102
1104
1106
1108
1110
890
880
870
860
850
840
Binding energy (eV)

*FIG. 11*

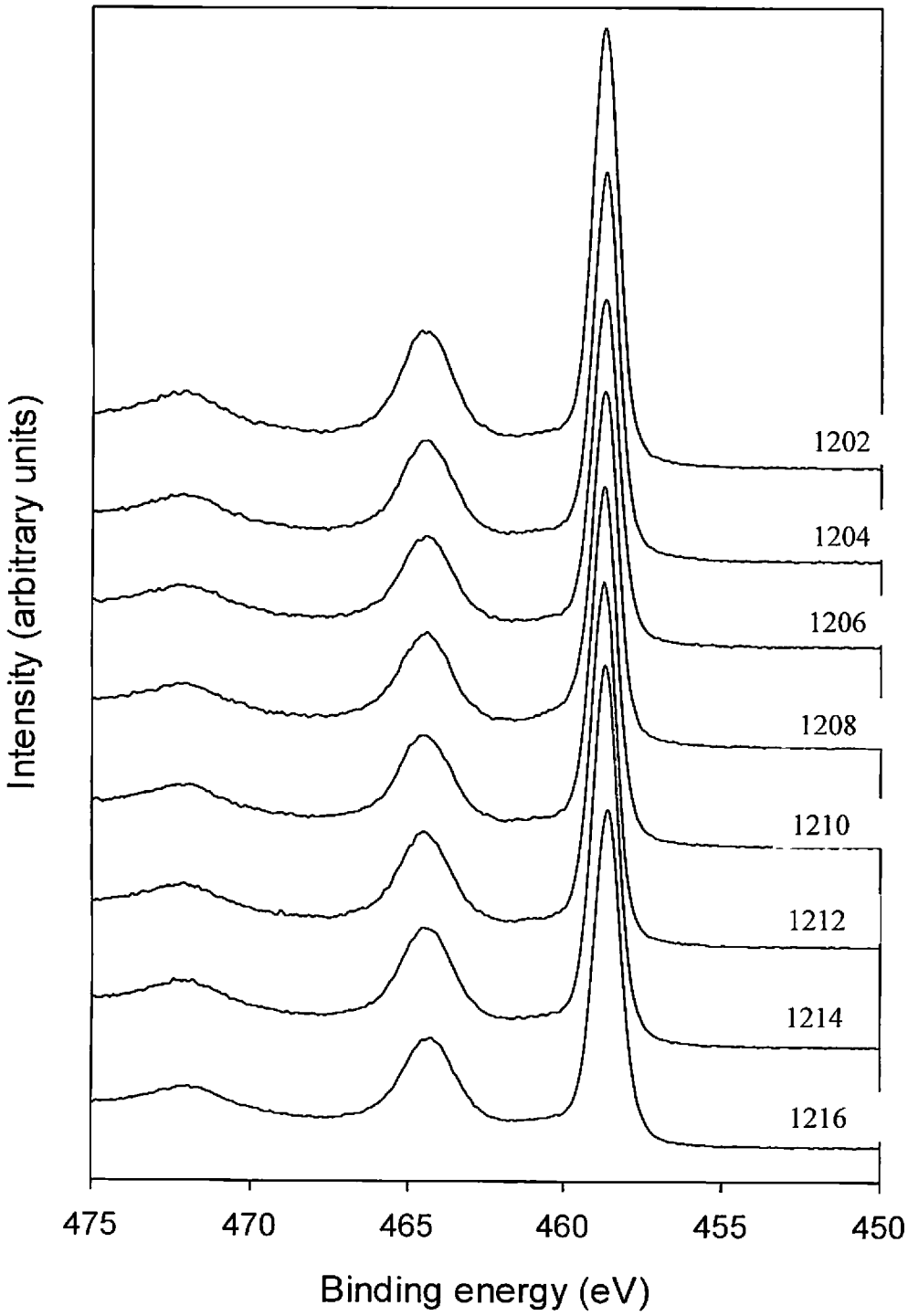
Intensity (arbitrary units)
1202
1204
1206
1208
1210
1212
1214
1216
475
470
465
460
455
450
Binding energy (eV)

*FIG. 12*

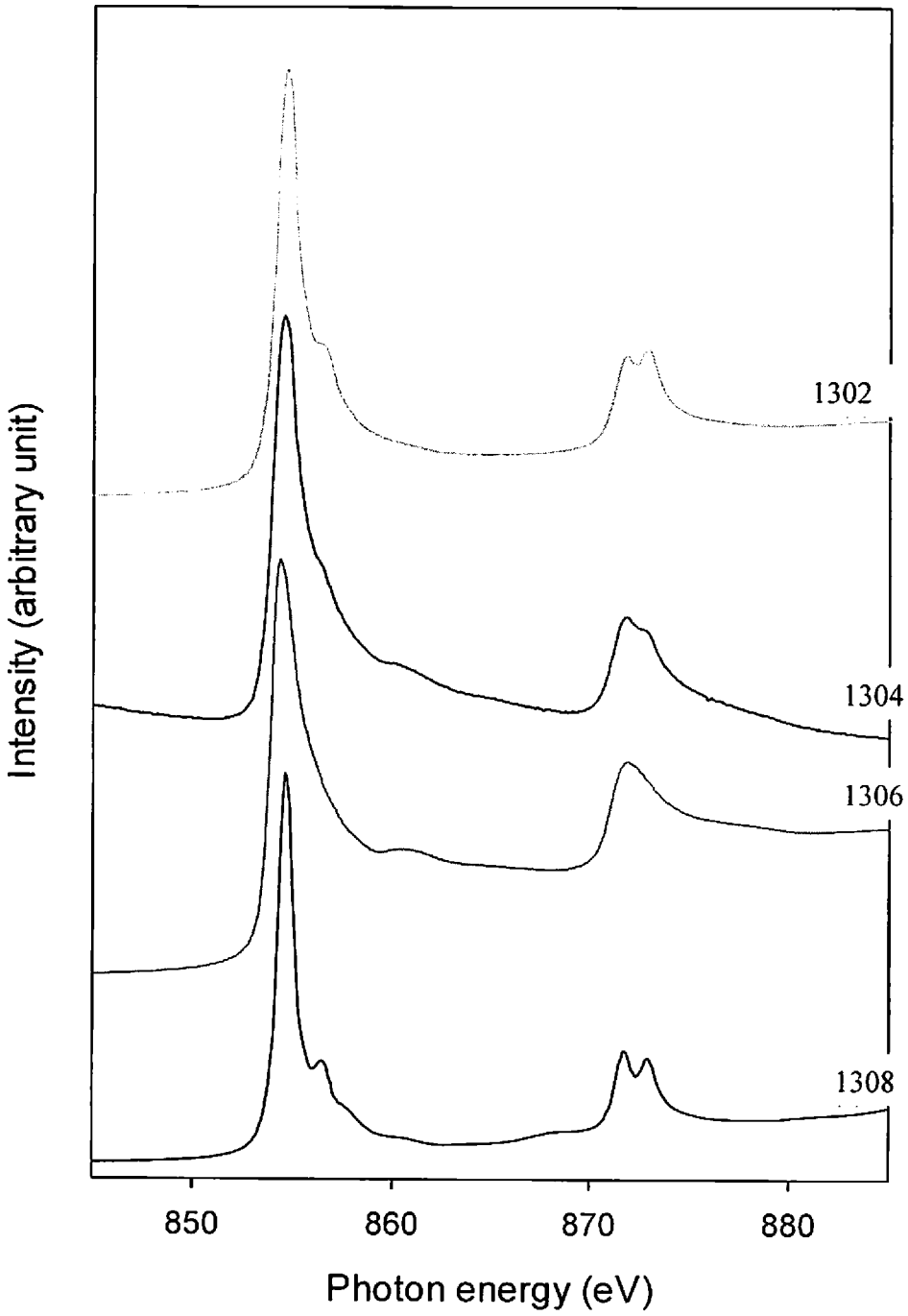
Intensity (arbitrary unit)
1302
1304
1306
1308
850
860
870
880
Photon energy (eV)

*FIG. 13*

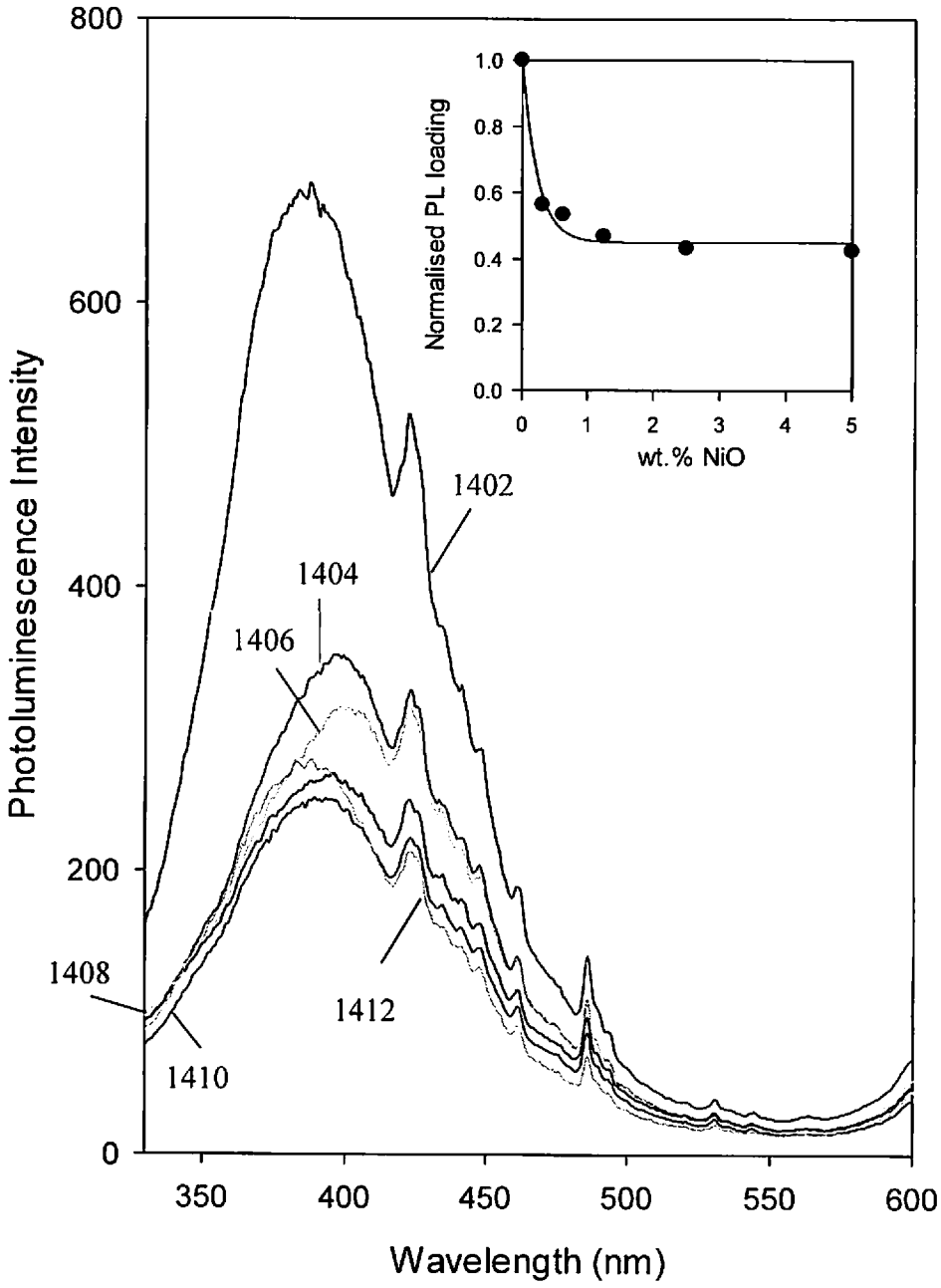
800
600
400
200
0
Photoluminescence Intensity
350
400
450
500
550
600
Wavelength (nm)
1402
1404
1406
1408
1410
1412
Normalised PL loading
1.0
0.8
0.6
0.4
0.2
0.0
0
1
2
3
4
5
wt.% NiO

*FIG. 14*

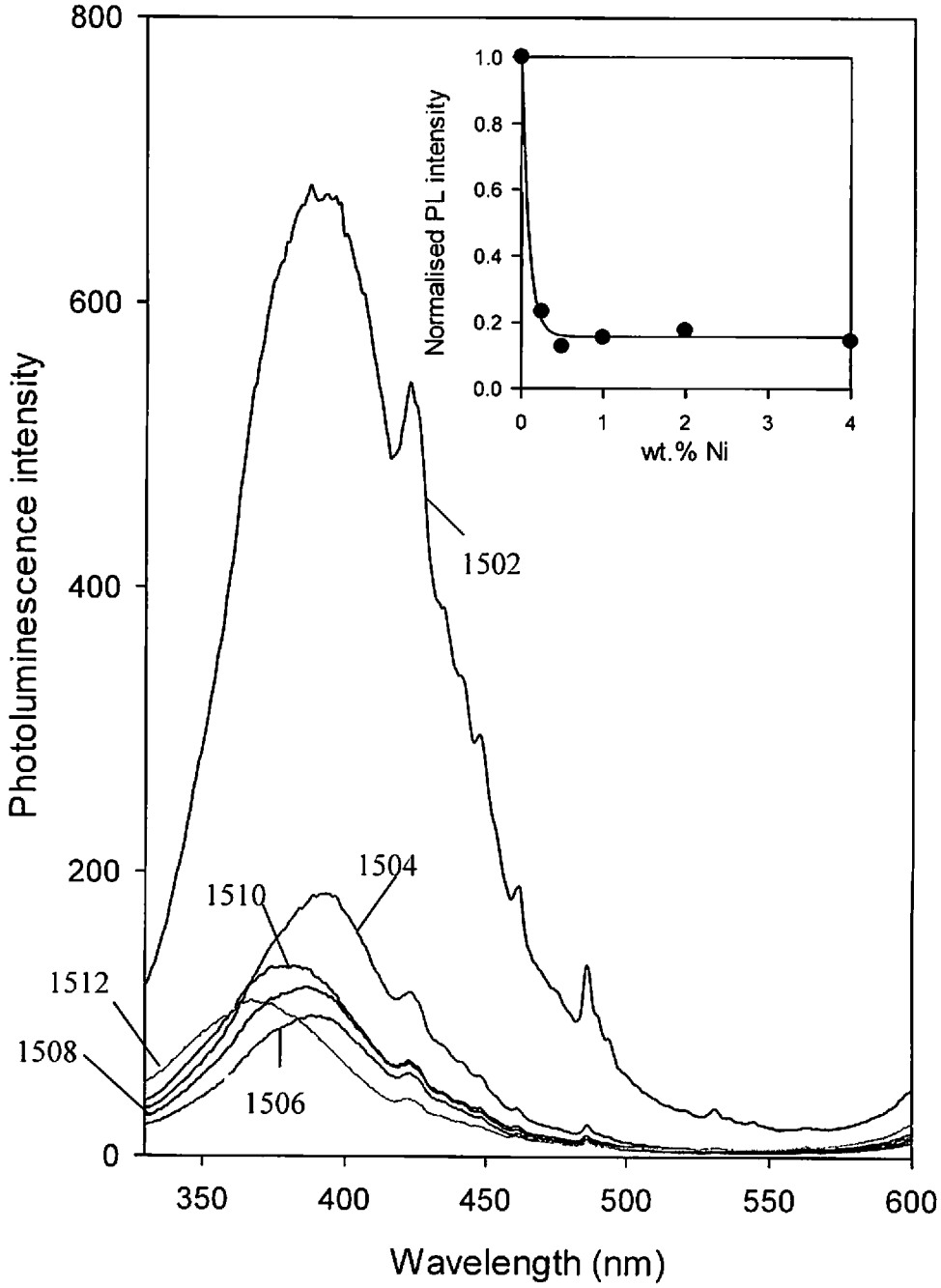
800
600
400
200
0
Photoluminescence intensity
350
400
450
500
550
600
Wavelength (nm)
1502
1504
1510
1512
1508
1506
Normalised PL intensity
1.0
0.8
0.6
0.4
0.2
0.0
0
1
2
3
4
wt.% Ni

*FIG. 15*

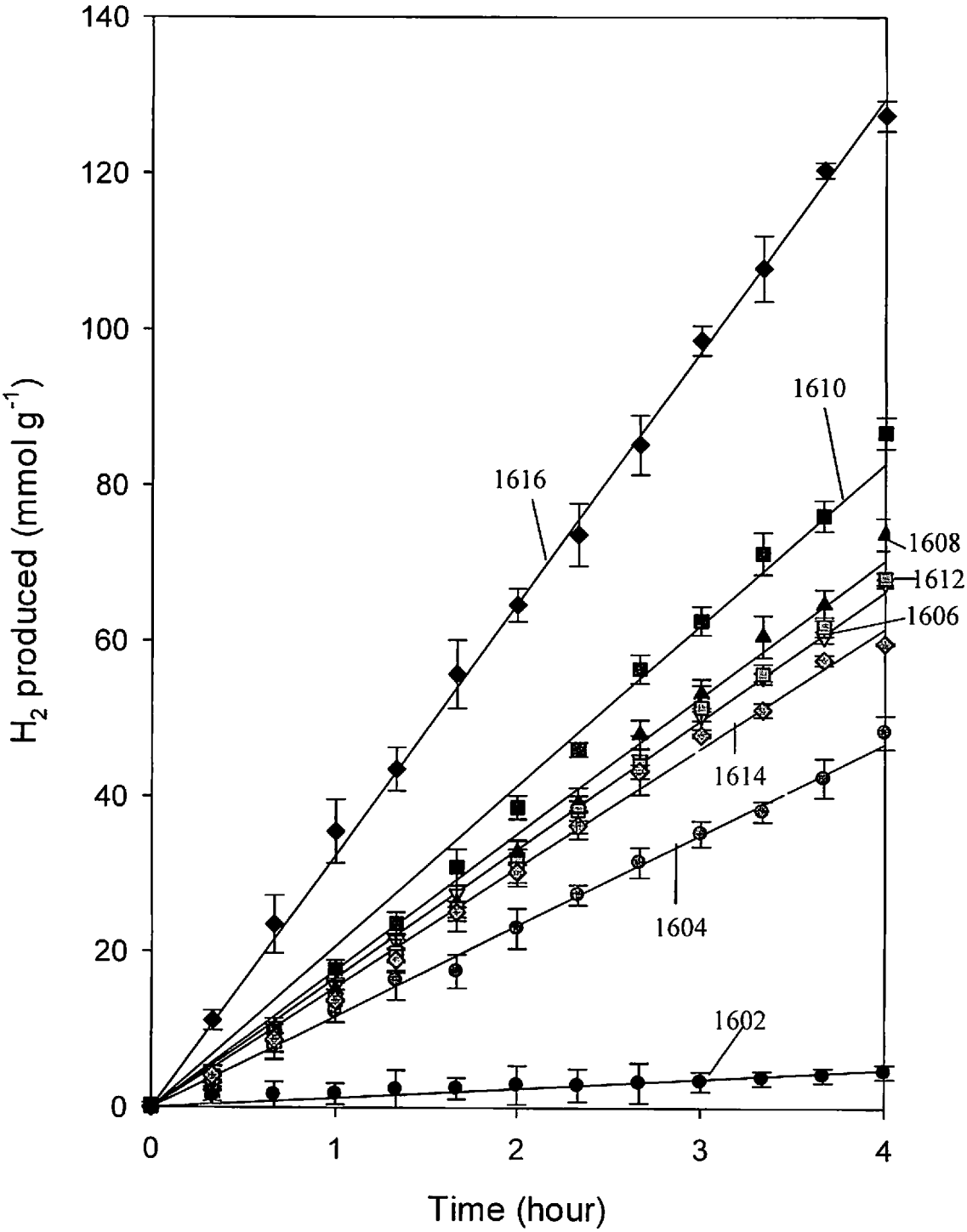
140
120
100
80
60
40
20
0
0
1
2
3
4
$H_2$ produced (mmol $g^{-1}$)
Time (hour)
1616
1610
1608
1612
1606
1614
1604
1602

*FIG. 16*

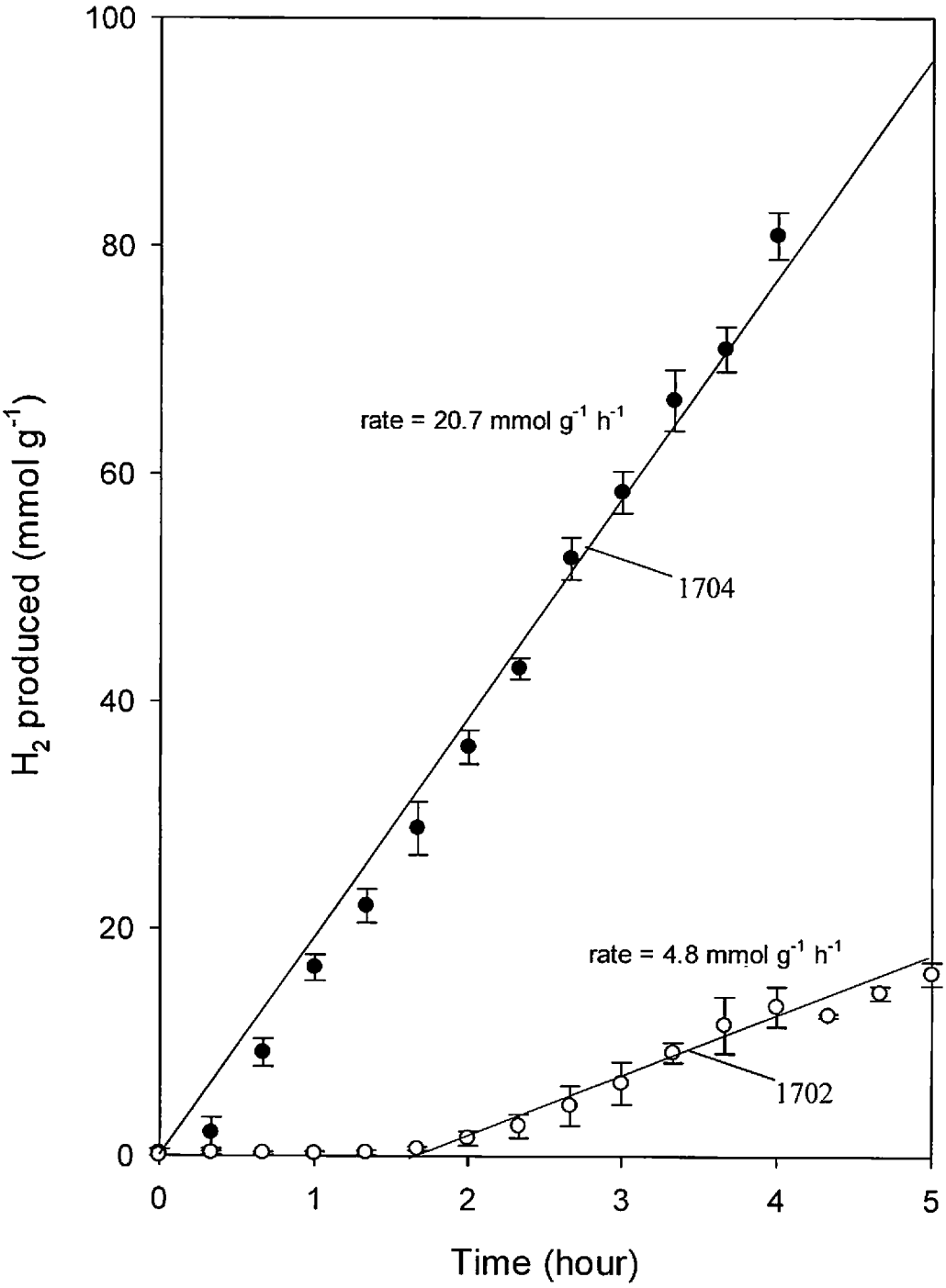
100
80
60
40
20
0
0
1
2
3
4
5
H2 produced (mmol g-1)
Time (hour)
rate = 20.7 mmol g-1 h-1
1704
rate = 4.8 mmol g-1 h-1
1702

*FIG. 17*

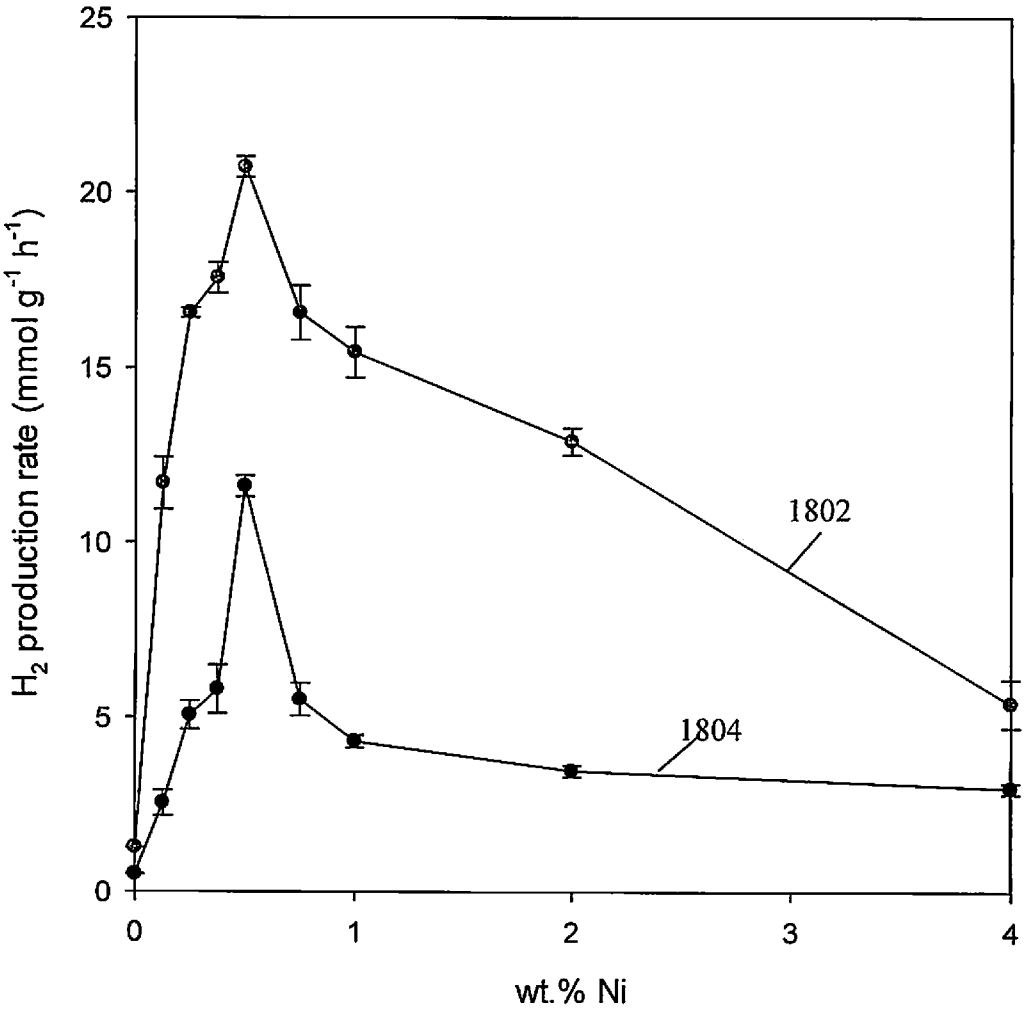
25
20
15
10
5
0
0
1
2
3
4
$H_2$ production rate (mmol $g^{-1}$ $h^{-1}$)
wt.% Ni
1802
1804

*FIG. 18*

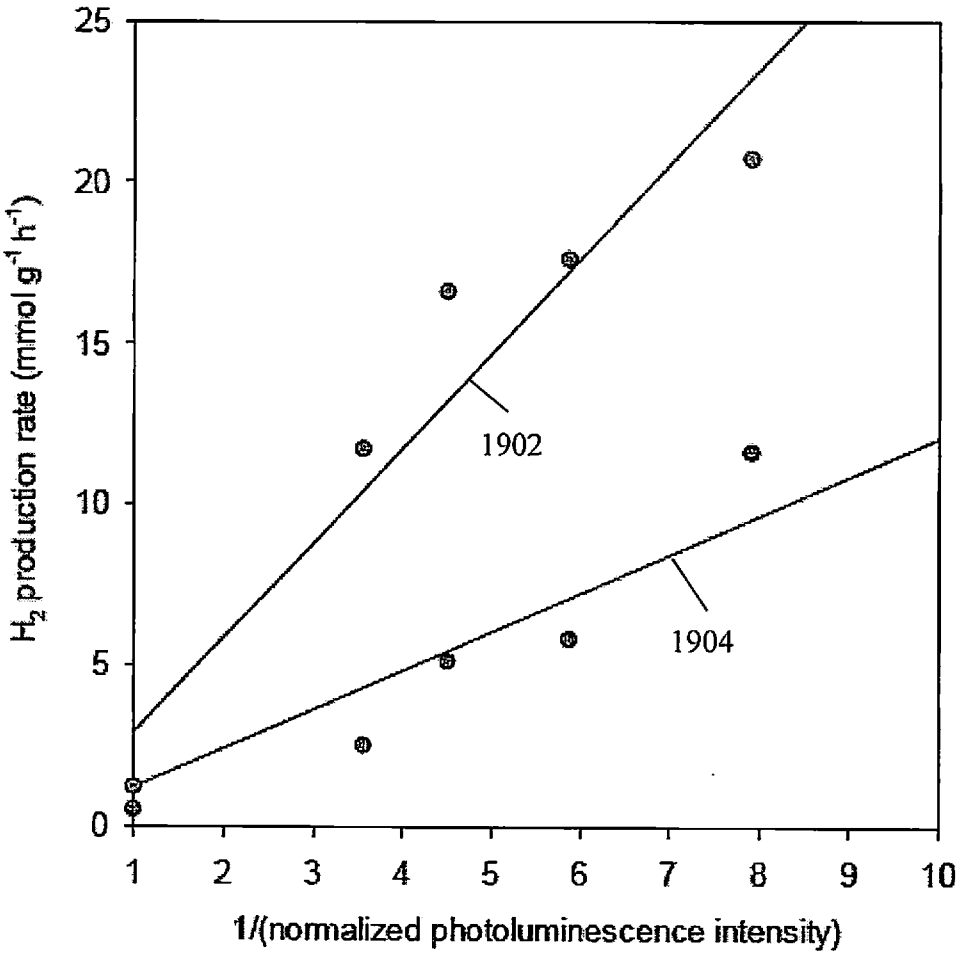
25
20
15
10
5
0
1
2
3
4
5
6
7
8
9
10
$H_2$ production rate (mmol $g^{-1}$ $h^{-1}$)
1/(normalized photoluminescence intensity)
1902
1904

*FIG. 19*

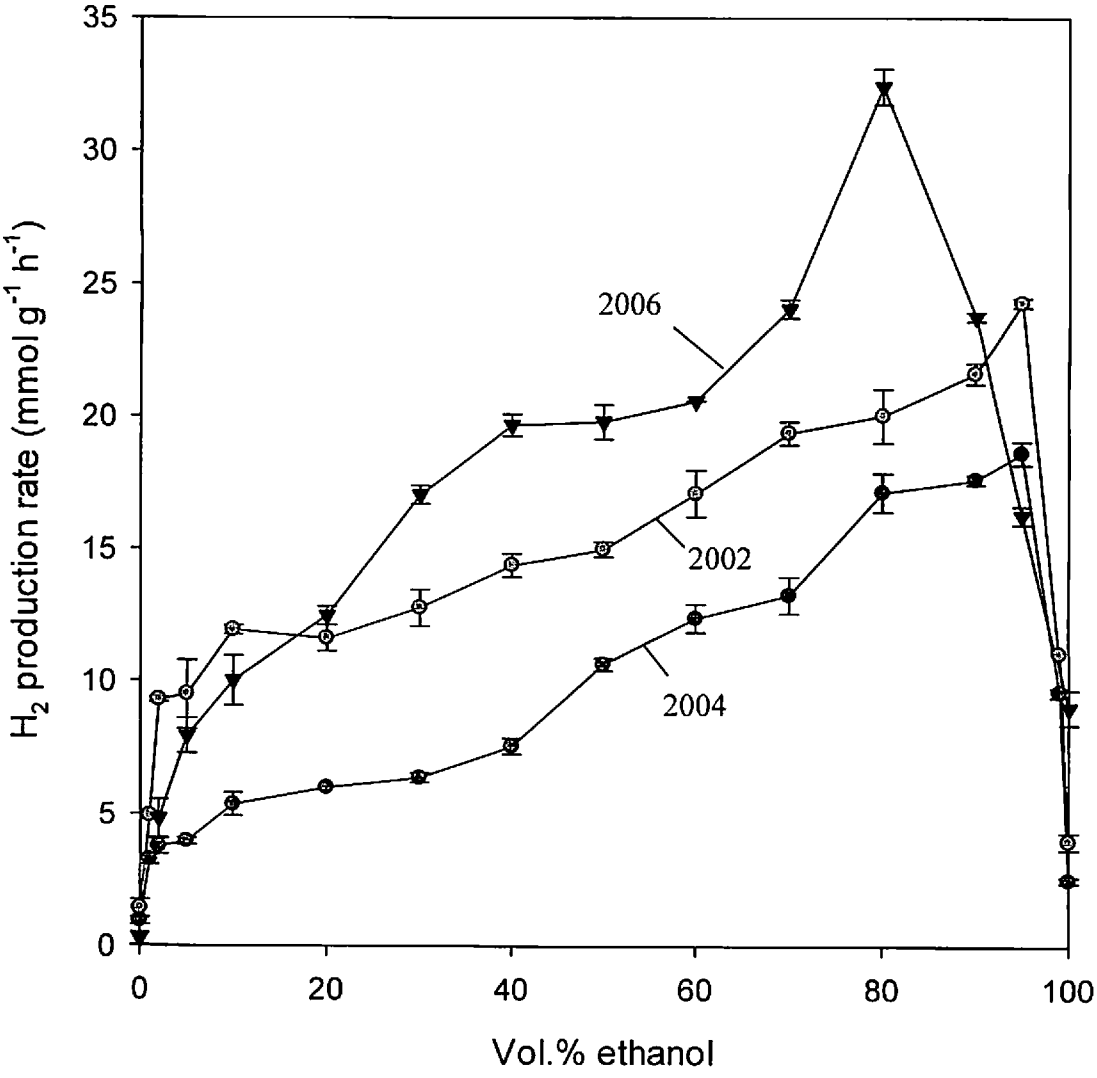
35
30
25
20
15
10
5
0
0
20
40
60
80
100
$H_2$ production rate (mmol $g^{-1}$ $h^{-1}$)
Vol.% ethanol
2006
2002
2004

*FIG. 20*

# INTERNATIONAL SEARCH REPORT

International application No
PCT/IB2016/051946

A. CLASSIFICATION OF SUBJECT MATTER
INV. C01G23/047 C01B3/04 B01J35/00 B01J21/06 B01J23/755
B01J35/02 B01J35/10 B01J37/03 B01J37/08
ADD.
According to International Patent Classification (IPC) or to both national classification and IPC

B. FIELDS SEARCHED

Minimum documentation searched (classification system followed by classification symbols)
C01G C01B B01J

Documentation searched other than minimum documentation to the extent that such documents are included in the fields searched

Electronic data base consulted during the international search (name of data base and, where practicable, search terms used)
EPO-Internal, WPI Data

C. DOCUMENTS CONSIDERED TO BE RELEVANT

| Category* | Citation of document, with indication, where appropriate, of the relevant passages | Relevant to claim No. |
|---|---|---|
| X | CHEN WAN-TING ET AL: "Ni/TiO2: A promising low-cost photocatalytic system for solar H2production from ethanol-water mixt", JOURNAL OF CATALYSIS, vol. 326, 5 April 2015 (2015-04-05), pages 43-53, XP029221717, ISSN: 0021-9517, DOI: 10.1016/J.JCAT.2015.03.008 the whole document figures; examples; tables -/-- | 1-20 |

[X] Further documents are listed in the continuation of Box C.

[X] See patent family annex.

* Special categories of cited documents :

"A" document defining the general state of the art which is not considered to be of particular relevance

"E" earlier application or patent but published on or after the international filing date

"L" document which may throw doubts on priority claim(s) or which is cited to establish the publication date of another citation or other special reason (as specified)

"O" document referring to an oral disclosure, use, exhibition or other means

"P" document published prior to the international filing date but later than the priority date claimed

"T" later document published after the international filing date or priority date and not in conflict with the application but cited to understand the principle or theory underlying the invention

"X" document of particular relevance; the claimed invention cannot be considered novel or cannot be considered to involve an inventive step when the document is taken alone

"Y" document of particular relevance; the claimed invention cannot be considered to involve an inventive step when the document is combined with one or more other such documents, such combination being obvious to a person skilled in the art

"&" document member of the same patent family

| Date of the actual completion of the international search | Date of mailing of the international search report |
|---|---|
| 28 July 2016 | 08/08/2016 |

| Name and mailing address of the ISA/ | Authorized officer |
|---|---|
| European Patent Office, P.B. 5818 Patentlaan 2<br>NL - 2280 HV Rijswijk<br>Tel. (+31-70) 340-2040,<br>Fax: (+31-70) 340-3016 | Holzwarth, Arnold |

3

Form PCT/ISA/210 (second sheet) (April 2005)

C(Continuation). DOCUMENTS CONSIDERED TO BE RELEVANT

| Category* | Citation of document, with indication, where appropriate, of the relevant passages | Relevant to claim No. |
|---|---|---|
| | & Wan-Ting Chen ET AL: "Supplementary information Ni/TiO 2 ; A Promising Low Cost Photocatalytic System for Solar H 2 Production from Ethanol-Water Mixtures", , 5 April 2015 (2015-04-05), XP055291640, Retrieved from the Internet: URL:http://www.sciencedirect.com/science/MiamiMultiMediaURL/1-s2.0-S0021951715000780/1-s2.0-S0021951715000780-mmc1.docx/272561/html/S0021951715000780/9b9ef222fdab5a5351d2054e05ed738f/mmc1.docx [retrieved on 2016-07-27] figures | |
| A | YOONG L S ET AL: "Development of copper-doped TiO2 photocatalyst for hydrogen production under visible light", ENERGY, PERGAMON PRESS, OXFORD, GB, vol. 34, no. 10, 15 August 2009 (2009-08-15), pages 1652-1661, XP026564647, ISSN: 0360-5442, DOI: 10.1016/J.ENERGY.2009.07.024 [retrieved on 2009-08-15] abstract page 1653 page 1659 figure 10; table 4 | 1-20 |
| X | EP 0 818 239 A1 (PETROLEUM ENERGY CENTER FOUND [JP]) 14 January 1998 (1998-01-14) column 6, line 27 - line 33; claims; examples 13-15 | 1-11 |
| A,P | WO 2016/005855 A1 (SABIC GLOBAL TECHNOLOGIES BV [NL]) 14 January 2016 (2016-01-14) the whole document | 1-20 |
| A,P | WO 2015/118424 A1 (SABIC GLOBAL TECHNOLOGIES BV [NL]) 13 August 2015 (2015-08-13) the whole document | 1-20 |
| A,P | WO 2015/056054 A1 (SAUDI BASIC IND CORP [SA]; IDRISS HICHAM [SA]) 23 April 2015 (2015-04-23) the whole document | 1-20 |

-/--

C(Continuation). DOCUMENTS CONSIDERED TO BE RELEVANT

| Category* | Citation of document, with indication, where appropriate, of the relevant passages | Relevant to claim No. |
|---|---|---|
| A | GAO YINA ET AL: "Controlled facile synthesis and photocatalytic activity of ultrafine high crystallinity TiO2nanocrystals with tunable anatase/rutile ratios", APPLIED SURFACE SCIENCE, vol. 294, 28 December 2013 (2013-12-28), pages 36-41, XP028611712, ISSN: 0169-4332, DOI: 10.1016/J.APSUSC.2013.12.107 the whole document ----- | 1-20 |

# INTERNATIONAL SEARCH REPORT

Information on patent family members

International application No
PCT/IB2016/051946

| Patent document cited in search report | Publication date | Patent family member(s) | Publication date |
|---|---|---|---|
| EP 0818239 A1 | 14-01-1998 | DE 69723924 D1 | 11-09-2003 |
| | | DE 69723924 T2 | 03-06-2004 |
| | | DE 69733503 D1 | 14-07-2005 |
| | | DE 69733503 T2 | 23-03-2006 |
| | | EP 0818239 A1 | 14-01-1998 |
| | | EP 1340540 A1 | 03-09-2003 |
| | | JP 3844823 B2 | 15-11-2006 |
| | | JP H09262482 A | 07-10-1997 |
| | | US 6077492 A | 20-06-2000 |
| | | WO 9726991 A1 | 31-07-1997 |
| WO 2016005855 A1 | 14-01-2016 | NONE | |
| WO 2015118424 A1 | 13-08-2015 | NONE | |
| WO 2015056054 A1 | 23-04-2015 | CN 105636901 A | 01-06-2016 |
| | | EP 3057906 A1 | 24-08-2016 |
| | | WO 2015056054 A1 | 23-04-2015 |